

Morphoelasticity of Large Bending Deformations of Cell Sheets during Development

Pierre A. Haas* and Raymond E. Goldstein†

Department of Applied Mathematics and Theoretical Physics, Centre for Mathematical Sciences,
University of Cambridge, Wilberforce Road, Cambridge CB3 0WA, United Kingdom

(Dated: August 16, 2022)

Deformations of cell sheets during morphogenesis are driven by developmental processes such as cell division and cell shape changes. In morphoelastic shell theories of development, these processes appear as variations of the intrinsic geometry of a thin elastic shell. However, morphogenesis often involves large bending deformations that are outside the formal range of validity of these shell theories. Here, by asymptotic expansion of three-dimensional incompressible morphoelasticity in the limit of a thin shell, we derive a shell theory for large intrinsic bending deformations and emphasise the resulting geometric material anisotropy and the elastic role of cell constriction. Taking the invagination of the green alga *Volvox* as a model developmental event, we show how results for this theory differ from those for a classical shell theory that is not formally valid for these large bending deformations and reveal how these geometric effects stabilise invagination.

I. INTRODUCTION

During animal and plant development, cell division, cell shape changes, and related processes can drive deformations of cell sheets [1–6]. In elastic continuum theories of the development of the green alga *Volvox* [7–10], of tissue folding in *Drosophila* [11, 12], or of more abstract active surfaces [13], these driving processes appear as changes of the reference or intrinsic geometry of thin elastic shells.

Just as classical thin shell theories arise from an asymptotic expansion of bulk elasticity in the small thickness of the shell [14–16], these “morphoelastic” shell theories should be asymptotic limits of a bulk theory. While there is now a well-established framework of three-dimensional morphoelasticity [17, 18], based on a multiplicative decomposition of the deformation gradient tensor into intrinsic and elastic deformations [19], studies of this asymptotic limit appear to have been restricted to the case of flat morphoelastic plates. Extensions of the classical Föppl–von Kármán equations [20, 21] have been derived for this case, but we are not aware of any corresponding study for curved morphoelastic shells. Rather, such studies have remained more phenomenological: some models [7, 8, 11–13] simply replaced the elastic strains in classical shell theories [15, 22, 23] with measures of the difference of the intrinsic and deformed geometries. Other studies [9, 10] took a more geometric approach, mirroring geometric derivations of classical shell theories [22] based on the so-called Kirchhoff “hypothesis”. This is the asymptotic result [15] that the normals of the midsurface of the undeformed shell remain, at leading order, normal to the deformed midsurface.

There is however one more serious limitation of these models: tissues in development undergo large bending deformations (Fig. 1) that are outside the formal range of validity of the underlying thin shell theories, which assume that the thickness of the shell is much smaller than all lengthscales of the midsurface of the shell [15, 22, 23]. However, even if the thickness of the cell sheet is much smaller than its undeformed radius of curvature, this radius of curvature may become comparable,

locally, to the thickness of the cell sheet as it deforms (Fig. 1). This is associated with cells contracting at one cell pole to splay and thereby bend the cell sheet [4].

Here, we derive a theory of thin incompressible morphoelastic shells undergoing large bending deformations by asymptotic expansion of three-dimensional elasticity. We reveal how, even in a constitutively isotropic material, this new scaling limit of large bending deformations induces, in the thin shell limit, a geometric anisotropy absent from classical shell theories: different deformation directions exhibit different deformation responses. We stress how this geometric effect is associated with the geometric singularity of cell constriction, i.e. the limit of wedged triangular cells [Fig. 1(b), inset] associated with these large bending deformations. Specialising to the invagination of the green alga *Volvox* [25, 26], we then

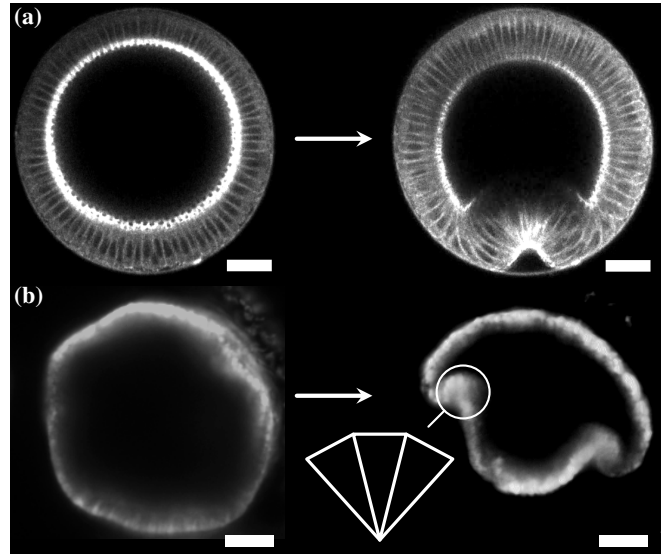


FIG. 1. Large bending deformations during morphogenesis: even if the thickness of the cell sheet is small compared to the undeformed radius of curvature, the local radius of curvature need not remain small compared to the cell sheet thickness as the sheet deforms. (a) Cross section of ventral furrow formation in *Drosophila*, reproduced from Ref. [24]. (b) Midsagittal cross section of invagination in the spherical alga *Volvox globator*, reproduced from Ref. [8]. Inset: cartoon of constricted triangular cells in the bend region. Scale bars: 20 μm .

* haas@maths.ox.ac.uk; current address: Mathematical Institute, University of Oxford, Woodstock Road, Oxford OX2 6GG, United Kingdom

† r.e.goldstein@damtp.cam.ac.uk

show how results for this theory differ from those for a classical theory that is not formally valid in this large bending limit, and reveal how invagination is stabilised by the geometry of large bending deformations.

II. ELASTIC MODEL

In this section, we describe large bending deformations of a thin incompressible morphoelastic shell, starting from three-dimensional morphoelasticity. We shall have to distinguish between three configurations of the shell [Fig. 2(a)]: (i) the undeformed configuration of the shell, (ii) the deformed configuration of the shell, and (iii) the intrinsic configuration of the shell that encodes the local, intrinsic deformations of the shell, i.e. the cell shape changes or cell division in the biological system. These intrinsic deformations are not in general compatible with the global geometry of the shell. Elasticity

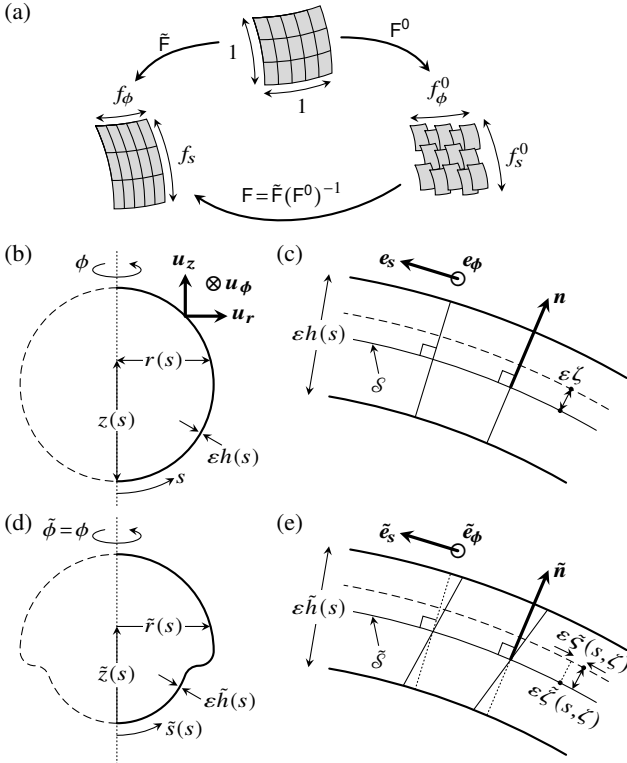


FIG. 2. Morphoelasticity of an axisymmetric shell. (a) The undeformed (top), deformed (left), and intrinsic (right) configurations of the shell are related by the three tensors $\tilde{\mathbf{F}}$, \mathbf{F}^0 , and $\mathbf{F} = \tilde{\mathbf{F}}(\mathbf{F}^0)^{-1}$. (b) Undeformed geometry of an axisymmetric shell of thickness εh , described by coordinates $r(s)$, $z(s)$, where s is arclength, with respect to the basis $\{\mathbf{u}_r, \mathbf{u}_\phi, \mathbf{u}_z\}$ of cylindrical polars. (c) Cross section of the undeformed shell, defining a local basis $\mathcal{B} = \{\mathbf{e}_s, \mathbf{e}_\phi, \mathbf{n}\}$ and the transverse coordinate ζ . (d) Deformed geometry of the shell: after a torsionless deformation, the shell has thickness $\varepsilon \tilde{h}$, arclength \tilde{s} , and is described by coordinates $\tilde{r}(s)$, $\tilde{z}(s)$ with respect to cylindrical polars. (e) Cross section of the deformed shell, defining a local basis $\tilde{\mathcal{B}} = \{\tilde{\mathbf{e}}_s, \tilde{\mathbf{e}}_\phi, \tilde{\mathbf{n}}\}$. Normals to the midsurface rotate so that a point at a distance $\varepsilon \zeta$ from the undeformed midsurface \mathcal{S} is at a distance $\varepsilon \tilde{\zeta}(s, \zeta)$ from the deformed midsurface $\tilde{\mathcal{S}}$, and displaced by a distance $\varepsilon \tilde{\zeta}(s, \zeta)$ parallel to $\tilde{\mathcal{S}}$.

must therefore intervene to “glue” the intrinsically deformed patches of cell sheet back together, as illustrated in Fig. 2(a). Configurations (i) and (ii) are related by the geometric deformation gradient $\tilde{\mathbf{F}}$. This tensor decomposes multiplicatively into an intrinsic contribution \mathbf{F}^0 that relates configurations (i) and (iii), and an elastic contribution $\mathbf{F} = \tilde{\mathbf{F}}(\mathbf{F}^0)^{-1}$. This is the multiplicative decomposition of morphoelasticity [17, 18].

In this section, we restrict to torsionless deformations of an axisymmetric shell. The analysis can be extended to more general deformations of the shell, and, for the sake of completeness, we do so in Appendix A, but the restriction to axisymmetric deformations eschews the mire of tensorial notation that arises in the general case.

The derivation of the shell theory for large bending deformations divides, like derivations of classical shell theories, into two steps: first, in subsection II A, we describe the kinematics of the deformations and derive expressions for the geometric, intrinsic, and elastic deformation gradients. Second, in subsection II B, we analyse the mechanics of the shell and expand the three-dimensional elastic energy and equilibrium conditions asymptotically. At the end of this section, in subsection II C, we discuss the limit of small bending deformations that gives rise to classical shell theories.

A. Axisymmetric deformations of an elastic shell

We consider an elastic shell of undeformed thickness εh , where $\varepsilon \ll 1$ is a small asymptotic parameter expressing the thinness of the shell compared to other lengthscales associated with its midsurface. Large bending deformations will be introduced by allowing one of the intrinsic radii of curvature of the shell to be of order $O(\varepsilon)$. We now derive an expression for the elastic deformation gradient \mathbf{F} for torsionless deformations of an axisymmetric shell.

1. Undeformed configuration of the shell

We shall describe the undeformed configuration \mathcal{V} of the shell with reference to a midsurface \mathcal{S} that we shall choose later. With respect to the basis $\{\mathbf{u}_r, \mathbf{u}_\phi, \mathbf{u}_z\}$ of cylindrical coordinates, we define the position vector of a point on \mathcal{S} ,

$$\boldsymbol{\rho}(s, \phi) = r(s)\mathbf{u}_r(\phi) + z(s)\mathbf{u}_z, \quad (1)$$

with s denoting arclength and ϕ being the azimuthal coordinate [Fig. 2(b)]. The tangent angle $\psi(s)$ of \mathcal{S} is defined by

$$r'(s) = \cos \psi(s), \quad z'(s) = \sin \psi(s), \quad (2)$$

in which dashes denote differentiation with respect to s . The vectors

$$\mathbf{e}_s(s, \phi) = \cos \psi(s)\mathbf{u}_r(\phi) + \sin \psi(s)\mathbf{u}_z, \quad \mathbf{e}_\phi(\phi) = \mathbf{u}_\phi(\phi) \quad (3)$$

thus constitute a basis of the tangent space of \mathcal{S} [Fig. 2(c)], which we extend to an orthonormal basis $\mathcal{B} = \{\mathbf{e}_s, \mathbf{e}_\phi, \mathbf{n}\}$ for \mathcal{V} by adjoining the normal to \mathcal{S} ,

$$\mathbf{n}(s, \phi) = \cos \psi(s)\mathbf{u}_z - \sin \psi(s)\mathbf{u}_r(\phi). \quad (4)$$

We complete the description of \mathcal{S} by computing its curvatures,

$$\kappa_s(s) = \psi'(s), \quad \kappa_\phi(s) = \frac{\sin \psi(s)}{r(s)}. \quad (5)$$

Now, the position of a point in \mathcal{V} is

$$\mathbf{r}(s, \phi, \zeta) = \boldsymbol{\rho}(s, \phi) + \varepsilon \zeta \mathbf{n}(s, \phi), \quad (6)$$

where we have introduced the transverse coordinate ζ [Fig. 2(c)]. Noting the partial derivatives $\partial \mathbf{n} / \partial s = \kappa_s \mathbf{e}_s$ and $\partial \mathbf{n} / \partial \phi = \kappa_\phi \mathbf{e}_\phi$, we obtain

$$\frac{\partial \mathbf{r}}{\partial s} = (1 - \varepsilon \kappa_s \zeta) \mathbf{e}_s, \quad \frac{\partial \mathbf{r}}{\partial \phi} = r(1 - \varepsilon \kappa_\phi \zeta) \mathbf{e}_\phi. \quad (7)$$

2. Deformed configuration of the shell

As the shell deforms into its deformed configuration $\tilde{\mathcal{V}}$, the midsurface \mathcal{S} maps to the deformed midsurface $\tilde{\mathcal{S}}$ [Fig. 2(d)], with position vector

$$\tilde{\boldsymbol{\rho}}(s, \phi) = \tilde{r}(s) \mathbf{u}_r(\phi) + \tilde{z}(s) \mathbf{u}_z, \quad (8)$$

where, in particular, s is again the undeformed arclength. Denoting by \tilde{s} the deformed arclength, we define the stretches

$$f_s(s) = \frac{d\tilde{s}}{ds}, \quad f_\phi(s) = \frac{\tilde{r}(s)}{r(s)}, \quad (9)$$

which enable us to define the tangent angle $\tilde{\psi}(s)$ of $\tilde{\mathcal{S}}$ by

$$\tilde{r}'(s) = f_s \cos \tilde{\psi}(s), \quad \tilde{z}'(s) = f_s \sin \tilde{\psi}(s), \quad (10)$$

where dashes still denote differentiation with respect to s . Similarly to the analysis of the undeformed configuration, we introduce the tangent vectors

$$\tilde{\mathbf{e}}_s(s, \phi) = \cos \tilde{\psi}(s) \mathbf{u}_r(\phi) + \sin \tilde{\psi}(s) \mathbf{u}_z, \quad \tilde{\mathbf{e}}_\phi(\phi) = \mathbf{u}_\phi(\phi), \quad (11)$$

and the normal vector

$$\tilde{\mathbf{n}}(s, \phi) = \cos \tilde{\psi}(s) \mathbf{u}_z - \sin \tilde{\psi}(s) \mathbf{u}_r(\phi) \quad (12)$$

to define an orthonormal basis $\tilde{\mathcal{B}} = \{\tilde{\mathbf{e}}_s, \tilde{\mathbf{e}}_\phi, \tilde{\mathbf{n}}\}$ to describe $\tilde{\mathcal{V}}$ [Fig. 2(e)]. The curvatures of the deformed shell are

$$\kappa_s(s) = \frac{\tilde{\psi}'(s)}{f_s(s)}, \quad \kappa_\phi(s) = \frac{\sin \tilde{\psi}(s)}{\tilde{r}(s)}. \quad (13)$$

As the shell deforms, the normals to \mathcal{S} need not remain normal to $\tilde{\mathcal{S}}$, and so a point in \mathcal{V} at a distance $\varepsilon \zeta$ from \mathcal{S} will end up, in $\tilde{\mathcal{V}}$, at a distance $\varepsilon \tilde{\zeta}$ from $\tilde{\mathcal{S}}$, and displaced by a distance $\varepsilon \tilde{\zeta}$ parallel to $\tilde{\mathcal{S}}$ [Fig. 2(e)]. By definition of the midsurface, $\tilde{\zeta} = \tilde{\zeta} = 0$ if $\zeta = 0$. The position of a point in $\tilde{\mathcal{V}}$ is thus

$$\tilde{\mathbf{r}}(s, \phi, \zeta) = \tilde{\boldsymbol{\rho}}(s, \phi) + \varepsilon \tilde{\zeta}(s, \zeta) \tilde{\mathbf{n}}(s, \phi) + \varepsilon \tilde{\zeta}(s, \zeta) \tilde{\mathbf{e}}_s(s, \phi). \quad (14)$$

Finally, using commata to denote partial differentiation, we note the partial derivatives

$$\frac{\partial \tilde{\mathbf{r}}}{\partial s} = [f_s (1 - \varepsilon \kappa_s \tilde{\zeta}) + \varepsilon \tilde{\zeta}_{,s}] \tilde{\mathbf{e}}_s + \varepsilon (\tilde{\zeta}_{,s} + f_s \kappa_s \tilde{\zeta}) \tilde{\mathbf{n}}, \quad (15a)$$

and

$$\frac{\partial \tilde{\mathbf{r}}}{\partial \phi} = [\tilde{r} (1 - \varepsilon \kappa_\phi \tilde{\zeta}) + \varepsilon \tilde{\zeta} \cos \tilde{\psi}] \tilde{\mathbf{e}}_\phi, \quad \varepsilon^{-1} \frac{\partial \tilde{\mathbf{r}}}{\partial \zeta} = \tilde{\zeta}_{,\zeta} \tilde{\mathbf{n}} + \tilde{\zeta}_{,\zeta} \tilde{\mathbf{e}}_s. \quad (15b)$$

3. Calculation of the deformation gradient tensors

Combining Eqs. (7) and (15), we obtain an expression for the geometric deformation gradient tensor and hence write down an expression for the intrinsic deformation gradient tensor, viz.

$$\tilde{\mathbf{F}} = \nabla_{\tilde{\mathbf{r}}} \tilde{\mathbf{r}} = \begin{pmatrix} \frac{f_s (1 - \varepsilon \kappa_s \tilde{\zeta}) + \varepsilon \tilde{\zeta}_{,s}}{1 - \varepsilon \kappa_s \tilde{\zeta}} & 0 & \tilde{\zeta}_{,\zeta} \\ 0 & \frac{f_\phi (1 - \varepsilon \kappa_\phi \tilde{\zeta}) + \varepsilon \tilde{\zeta} \cos \tilde{\psi} / r}{1 - \varepsilon \kappa_\phi \tilde{\zeta}} & 0 \\ \frac{\varepsilon (\tilde{\zeta}_{,s} + f_s \kappa_s \tilde{\zeta})}{1 - \varepsilon \kappa_s \tilde{\zeta}} & 0 & \tilde{\zeta}_{,\zeta} \end{pmatrix}, \quad \mathbf{F}^0 = \begin{pmatrix} \frac{f_s^0 (1 - \varepsilon \kappa_s^0 \zeta^0)}{1 - \varepsilon \kappa_s \zeta} & 0 & 0 \\ 0 & \frac{f_\phi^0 (1 - \varepsilon \kappa_\phi^0 \zeta^0)}{1 - \varepsilon \kappa_\phi \zeta} & 0 \\ \frac{\varepsilon \zeta_{,s}^0}{1 - \varepsilon \kappa_s \zeta} & 0 & \zeta_{,\zeta}^0 \end{pmatrix}, \quad (16)$$

In the expression for \mathbf{F}^0 , we have introduced the intrinsic stretches f_s^0, f_ϕ^0 , the intrinsic curvatures $\kappa_s^0, \kappa_\phi^0$, and the intrinsic displacement ζ^0 from the intrinsic midsurface \mathcal{S}^0 of the intrinsic configuration \mathcal{V}^0 of the shell. In writing down this expression for \mathbf{F}^0 , we have assumed that there is no intrinsic displacement parallel to the midsurface, $\zeta^0 = 0$. In Eq. (16), $\tilde{\mathbf{F}}$ is expressed with respect to the mixed basis $\tilde{\mathcal{B}} \otimes \mathcal{B}$, while \mathbf{F}^0 is expressed with respect to another mixed basis, $\mathcal{B}^0 \otimes \mathcal{B}$, where $\mathcal{B}^0 = \{\mathbf{E}_s, \mathbf{E}_\phi, \mathbf{N}\}$ is a (local) orthonormal basis for the intrinsically deformed configuration of the shell. The elastic deformation gradient is thus

$$\mathbf{F} = \tilde{\mathbf{F}}(\mathbf{F}^0)^{-1} = \begin{pmatrix} \frac{f_s(1 - \varepsilon\kappa_s\tilde{\zeta}) + \varepsilon(\tilde{\zeta}_{,s} + \tilde{\zeta}_{,\zeta^0}\zeta_{,s}^0)}{f_s^0(1 - \varepsilon\kappa_s^0\zeta^0)} & 0 & \tilde{\zeta}_{,\zeta^0} \\ 0 & \frac{f_\phi(1 - \varepsilon\kappa_\phi\tilde{\zeta}) + \varepsilon\tilde{\zeta}\cos\tilde{\psi}/r}{f_\phi^0(1 - \varepsilon\kappa_\phi^0\zeta^0)} & 0 \\ \frac{\varepsilon(\tilde{\zeta}_{,s} + f_s\kappa_s\tilde{\zeta}_{,s} - \zeta_{,s}^0\tilde{\zeta}_{,\zeta^0})}{f_s^0(1 - \varepsilon\kappa_s^0\zeta^0)} & 0 & \tilde{\zeta}_{,\zeta^0} \end{pmatrix}, \quad (17)$$

expressed here with respect to the natural mixed basis $\tilde{\mathcal{B}} \otimes \mathcal{B}^0$. Since $\tilde{\mathcal{B}}$ and \mathcal{B}^0 are orthonormal, there exists a rotation, represented by an orthogonal matrix \mathbf{R} , that maps $\tilde{\mathcal{B}}$ onto \mathcal{B}^0 . With respect to $\mathcal{B}^0 \otimes \mathcal{B}^0$, the elastic deformation gradient tensor is then represented by the matrix $\mathbf{R}\mathbf{F}$. This rotation can, as explained below, be in fact ignored in the calculations that follow. This simplification is not however possible for general deformations, as discussed in Appendix A.

B. Thin shell theory for large bending deformations

In this subsection, we derive the effective elastic energy for the shell by asymptotic expansion of three-dimensional elasticity. We assume the simplest constitutive law, that the shell is made of an incompressible neo-Hookean material [17], so that its elastic energy is

$$\mathcal{E} = \int_{\mathcal{V}^0} e \, dV^0, \quad \text{with } e = \frac{C}{2}(\mathcal{I}_1 - 3), \quad (18)$$

wherein C is a material parameter, and \mathcal{I}_1 is the first invariant of the right Cauchy–Green tensor $\mathbf{C} = \mathbf{F}^\top \mathbf{F}$ [17]. We emphasise that the integration of the strain energy density e is over the intrinsic configuration \mathcal{V}^0 of the shell, which has volume element dV^0 . The (first) Piola–Kirchhoff stress tensor for this neo–Hookean material [21] is, with respect to $\mathcal{B}^0 \otimes \mathcal{B}^0$,

$$\mathbf{P} = C[(\mathbf{R}\mathbf{F}) - p(\mathbf{R}\mathbf{F})^{-\top}] = \mathbf{C}\mathbf{R}\mathbf{Q}, \quad (19)$$

with $\mathbf{Q} = \mathbf{F} - p\mathbf{F}^{-\top}$, and where the Lagrange multiplier p is proportional to pressure and imposes the incompressibility condition $\det \mathbf{F} = 1$. The second equality follows, since \mathbf{R} is orthogonal, from $(\mathbf{R}\mathbf{F})^{-\top} = (\mathbf{F}^\top \mathbf{R}^\top)^{-1} = (\mathbf{F}^\top \mathbf{R}^{-1})^{-1} = \mathbf{R}\mathbf{F}^{-\top}$.

The configuration of the shell minimising the energy \mathcal{E} in Eq. (18) is determined by $\text{Div}^0 \mathbf{P} = \mathbf{0}$ [17], where the divergence is taken with respect to \mathcal{V}^0 . Separating into components parallel and perpendicular to the midsurface and using Eq. (19),

$$(\mathbf{Q}\mathbf{N})_{,\zeta^0} + \varepsilon \mathbf{R}^\top \nabla^0 \cdot (\mathbf{R}\mathbf{Q}\mathbf{J}) = \mathbf{0}, \quad (20)$$

since \mathbf{R} is independent of ζ^0 and orthogonal, where the nabla operator denotes the gradient on \mathcal{S}^0 , and where $\mathbf{J} = \mathbf{I} - \mathbf{N} \otimes \mathbf{N}$ denotes projection onto the intrinsic midsurface, normal to \mathbf{N} .

1. Scaling assumptions

We now introduce large intrinsic bending deformations explicitly by scaling the intrinsic curvatures so as to allow small

radii of curvature in the meridional direction, viz.

$$\kappa_s^0 = f_s^0 f_\phi^0 \frac{\lambda_s^0}{\varepsilon}, \quad \kappa_\phi^0 = f_s^0 f_\phi^0 \lambda_\phi^0, \quad (21)$$

wherein the rescaling by the prefactor $f_s^0 f_\phi^0$ absorbs, as do similar rescalings below, the intrinsic stretching of the midsurface. This scaling regime in which the meridional intrinsic curvature becomes comparable to the thickness of the cell sheet is the one relevant for *Volvox* invagination, as shown in Fig. 1(b). Appendix A treats the general case in which all components of the curvature tensor are allowed to be large.

Next, we make the standard scaling assumption of shell theory, that the elastic strains are small, i.e. that the stretches and curvatures in the deformed configuration do not differ “too much” from the intrinsic stretches and curvatures. More formally, we introduce the shell strains E_s, E_ϕ by writing

$$f_s = f_s^0(1 + \varepsilon E_s), \quad f_\phi = f_\phi^0(1 + \varepsilon E_\phi), \quad (22)$$

and the curvature strains L_s, L_ϕ by letting

$$\kappa_s = f_s^0 f_\phi^0 \left(\frac{\lambda_s^0}{\varepsilon} + L_s \right), \quad \kappa_\phi = f_s^0 f_\phi^0 \left(\lambda_\phi^0 + L_\phi \right). \quad (23)$$

Finally, we introduce the scaled variables

$$\mathbf{Z}^0 = f_s^0 f_\phi^0 \zeta^0, \quad \mathbf{Z} = f_s^0 f_\phi^0 \tilde{\zeta}, \quad \mathbf{S} = f_s^0 f_\phi^0 \tilde{\zeta}. \quad (24)$$

2. Boundary and incompressibility conditions

We now impose the incompressibility condition $\det \mathbf{F} = 1$ and the boundary conditions, which require that there be no external forces on the surfaces of the shell. These boundary conditions are relevant for many problems in developmental biology, where deformations are, as discussed in the introduction, driven by changes of the intrinsic geometry only; including external forces does not pose any additional difficulty, though.

These force-free boundary conditions read $\mathbf{P}^\pm \mathbf{N}_\pm = \mathbf{0}$ [17], where, from Eq. (19), $\mathbf{P}^\pm = \mathbf{C}\mathbf{R}\mathbf{Q}^\pm$ are the Piola–Kirchhoff stress tensors evaluated on the shell surfaces of the intrinsic configuration \mathcal{V}^0 , and \mathbf{N}_\pm are the unit outward normals to these shell surfaces. Since the rotation \mathbf{R} is an isometry, the boundary conditions become $\mathbf{Q}^\pm \mathbf{N}_\pm = \mathbf{0}$.

To complete the derivation of the boundary conditions, we must obtain expressions for the normals \mathbf{N}_\pm to the shell surfaces. At this stage, we complete specifying the midsurface by

choosing \mathcal{S}^0 so that the shell surfaces are at $\zeta^0 = \pm h^0/2$. Similarly to the calculations leading up to Eqs. (15), we compute the unit tangent vectors to the shell surfaces in the intrinsic configuration,

$$\mathbf{E}_s^\pm \parallel f_s^0 \left(1 \mp \varepsilon \kappa_s^0 h^0/2 \right) \mathbf{E}_s \pm \left(\varepsilon h_{,s}^0/2 \right) \mathbf{N}, \quad \mathbf{E}_\phi^\pm = \mathbf{E}_\phi, \quad (25)$$

expressed here with respect to $\mathcal{B}^0 = \{\mathbf{E}_s, \mathbf{E}_\phi, \mathbf{N}\}$. By definition, $\mathbf{N}_\pm \parallel \mathbf{E}_s^\pm \times \mathbf{E}_\phi^\pm$. Introducing a normalisation factor and expanding while recalling that $\kappa_s^0 = O(\varepsilon^{-1})$, we obtain

$$\begin{aligned} \mathbf{N}_\pm &= \pm \frac{\mathbf{N} \mp \nu_\pm \mathbf{E}_s}{\sqrt{1 + \nu_\pm^2}} \quad \text{with } \nu_\pm = \frac{\varepsilon h_{,s}^0/2}{f_s^0 (1 \mp \varepsilon \kappa_s^0 h^0/2)}, \\ &= \pm \mathbf{N} - \frac{\varepsilon h_{,s}^0}{f_s^0 (2 \mp f_s^0 f_\phi^0 \lambda_s^0 h^0)} \mathbf{E}_s + O(\varepsilon^2). \end{aligned} \quad (26)$$

3. Expansion of the boundary and incompressibility conditions

To expand the incompressibility and boundary conditions in the small parameter ε , we now posit regular expansions

$$Z = Z^0 + Z_{(0)} + \varepsilon Z_{(1)} + O(\varepsilon^2), \quad S = S_{(0)} + O(\varepsilon), \quad (27)$$

for the scaled transverse and parallel displacements. Throughout this paper, we shall use subscripts in parentheses in this way to denote the different terms in asymptotic expansions in ε . We further expand

$$\mathbf{Q} = \mathbf{Q}_{(0)} + \varepsilon \mathbf{Q}_{(1)} + O(\varepsilon^2), \quad p = p_{(0)} + O(\varepsilon). \quad (28)$$

a. Solution at order $O(1)$. At leading order, Eq. (20) yields $(\mathbf{Q}_{(0)} \mathbf{N})_{,\zeta^0} = \mathbf{0}$, so $\mathbf{Q}_{(0)} \mathbf{N} = \mathbf{Q}(s)$ is independent of ζ^0 . It follows that $\mathbf{0} = \mathbf{Q}^\pm \mathbf{N}_\pm = \pm \mathbf{Q}_{(0)}^\pm \mathbf{N} + O(\varepsilon) = \pm \mathbf{Q} + O(\varepsilon)$ using Eq. (26). Thus $\mathbf{0} \equiv \mathbf{Q} = \mathbf{Q}_{(0)} \mathbf{N} = (t_{(0)}^s, 0, t_{(0)}^n)$, where [27]

$$0 = t_{(0)}^s = \frac{\lambda_s^0 S_{(0)} \left[(S_{(0),Z^0})^2 - p_{(0)} (Z_{(0),Z^0})^2 \right] - S_{(0),Z^0} (1 + Z_{(0),Z^0}) [1 - \lambda_s^0 (Z^0 + Z_{(0)})]}{\lambda_s^0 S_{(0)} S_{(0),Z^0} - (1 + Z_{(0),Z^0}) [1 - \lambda_s^0 (Z^0 + Z_{(0)})]}, \quad (29a)$$

$$0 = t_{(0)}^n = \frac{\lambda_s^0 S_{(0)} S_{(0),Z^0} (1 + Z_{(0),Z^0}) (Z^0 + Z_{(0)}) - [1 - \lambda_s^0 (Z^0 + Z_{(0)})] [(1 + Z_{(0),Z^0})^2 - p_{(0)}]}{\lambda_s^0 S_{(0)} S_{(0),Z^0} - (1 + Z_{(0),Z^0}) [1 - \lambda_s^0 (Z^0 + Z_{(0)})]}. \quad (29b)$$

Moreover, expanding the incompressibility condition, we find

$$1 = \det \mathbf{F} = 1 + \frac{Z_{(0),Z^0} - \lambda_s^0 [S_{(0)} S_{(0),Z^0} + Z_{(0)} + (Z^0 + Z_{(0)}) Z_{(0),Z^0}]}{1 - \lambda_s^0 Z^0} + O(\varepsilon). \quad (30)$$

Eqs. (29) and (30) define a system of three simultaneous linear algebraic equations for $p_{(0)}$, $Z_{(0),Z^0}$, and $S_{(0),Z^0}$, with solution

$$p_{(0)} = \frac{(1 - \lambda_s^0 Z^0)^2}{[1 - \lambda_s^0 (Z^0 + Z_{(0)})]^2 + (\lambda_s^0 S_{(0)})^2}, \quad (31a)$$

$$Z_{(0),Z^0} = \frac{\lambda_s^0 \{ Z_{(0)} - \lambda_s^0 [S_{(0)}^2 + Z_{(0)} (Z^0 + Z_{(0)})] \}}{[1 - \lambda_s^0 (Z^0 + Z_{(0)})]^2 + (\lambda_s^0 S_{(0)})^2}, \quad (31b)$$

$$S_{(0),Z^0} = -\frac{\lambda_s^0 S_{(0)} (1 - \lambda_s^0 Z^0)}{[1 - \lambda_s^0 (Z^0 + Z_{(0)})]^2 + (\lambda_s^0 S_{(0)})^2}. \quad (31c)$$

Eqs. (31b) and (31c) imply

$$\begin{aligned} &-2(1 + Z_{(0),Z^0}) [1 - \lambda_s^0 (Z^0 + Z_{(0)})] + 2\lambda_s^0 S_{(0)} S_{(0),Z^0} \\ &= -2(1 - \lambda_s^0 Z^0). \end{aligned} \quad (32a)$$

Integrating using the fact that $Z_{(0)} = S_{(0)} = 0$ at $Z^0 = 0$ by definition of the midsurface, we obtain

$$[1 - \lambda_s^0 (Z^0 + Z_{(0)})]^2 + (\lambda_s^0 S_{(0)})^2 = (1 - \lambda_s^0 Z^0)^2. \quad (32b)$$

Eq. (31a) now becomes $p_{(0)} = 1$. Moreover, on substituting Eq. (32b) into Eq. (31b),

$$\frac{\partial Z_{(0)}}{\partial Z^0} = -\frac{\lambda_s^0 Z_{(0)}}{1 - \lambda_s^0 Z^0} \implies \frac{Z_{(0)}}{1 - \lambda_s^0 Z^0} = \text{const.}, \quad (33)$$

which, using $Z_{(0)} = 0$ at $Z^0 = 0$ again, yields $Z_{(0)} \equiv 0$. Hence $S_{(0)} \equiv 0$ from Eq. (31c). The last equality is the Kirchhoff ‘‘hypothesis’’ [15]: normals to the intrinsic midsurface remain, at lowest order, normal to the deformed midsurface.

b. Solution at orders $O(\varepsilon)$ and $O(\varepsilon^2)$. We now expand the incompressibility condition further, finding

$$\begin{aligned} 0 &= \det \mathbf{F} - 1 \\ &= \varepsilon \left(E_s + E_\phi - L_\phi Z^0 + \frac{\partial Z_{(1)}}{\partial Z^0} - \frac{L_s Z^0 + \lambda_s^0 Z_{(1)}}{1 - \lambda_s^0 Z^0} \right) + O(\varepsilon^2). \end{aligned} \quad (34)$$

On solving the resulting differential equation for $Z_{(1)}$ by imposing $Z_{(1)} = 0$ at $Z^0 = 0$, we obtain

$$Z_{(1)} = -\frac{Z^0 \{ 6(E_s + E_\phi) - 3Z^0 [L_s + L_\phi + \lambda_s^0 (E_s + E_\phi)] + 2\lambda_s^0 L_\phi (Z^0)^2 \}}{6(1 - \lambda_s^0 Z^0)}. \quad (35)$$

Next, we formally expand the entries of the deformation gradient in Eq. (17) further by writing

$$\mathbf{F} = \begin{pmatrix} 1 + \varepsilon a_{(1)} + \varepsilon^2 a_{(2)} + O(\varepsilon^3) & 0 & \varepsilon v_{(1)} + O(\varepsilon^2) \\ 0 & 1 + \varepsilon b_{(1)} + \varepsilon^2 b_{(2)} + O(\varepsilon^3) & 0 \\ \varepsilon w_{(1)} + O(\varepsilon^2) & 0 & 1 + \varepsilon c_{(1)} + \varepsilon^2 c_{(2)} + O(\varepsilon^3) \end{pmatrix}. \quad (36)$$

In particular, we obtain

$$a_{(1)} = \frac{6E_s - 6 [L_s + \lambda_s^0 (E_s - E_\phi)] Z^0 + 3\lambda_s^0 [L_s - L_\phi + \lambda_s^0 (E_s - E_\phi)] (Z^0)^2 + 2(\lambda_s^0)^2 L_\phi (Z^0)^3}{6(1 - \lambda_s^0 Z^0)^2}, \quad b_{(1)} = E_\phi - Z^0 L_\phi. \quad (37)$$

Expressions for $a_{(2)}$, $b_{(2)}$, $c_{(1)}$, $c_{(2)}$, $v_{(1)}$, $w_{(1)}$ can be obtained in terms of the expansions (27), but will turn out to be of no consequence. Hence the incompressibility condition becomes

$$1 = \det \mathbf{F} = 1 + \varepsilon (a_{(1)} + b_{(1)} + c_{(1)}) + \varepsilon^2 (a_{(2)} + b_{(2)} + c_{(2)} + a_{(1)}b_{(1)} + b_{(1)}c_{(1)} + c_{(1)}a_{(1)} - v_{(1)}w_{(1)}) + O(\varepsilon^3). \quad (38)$$

Next, we notice that $\mathbf{Q}_{(0)} = \mathbf{O}$ from Eq. (36), and hence Eq. (20) at order $O(\varepsilon)$ is just $(\mathbf{Q}_{(1)}\mathbf{N})_{,\zeta^0} = \mathbf{0}$. Moreover, since $\mathbf{Q}_{(0)} = \mathbf{O}$ and using Eq. (26), $\mathbf{0} = \mathbf{Q}^\pm \mathbf{N} = \varepsilon \mathbf{Q}_{(1)}^\pm \mathbf{N} + O(\varepsilon^2)$, so, similarly to above, $\mathbf{Q}_{(1)}\mathbf{N} \equiv \mathbf{0}$. Now, on direct computation of $\mathbf{Q}_{(1)}$ from Eq. (36), we find $\mathbf{Q}_{(1)}\mathbf{N} = (\varepsilon(v_{(1)} + w_{(1)}), 0, O(\varepsilon))$. From this and from Eq. (38), we infer

$$w_{(1)} = -v_{(1)}, \quad c_{(1)} = -(a_{(1)} + b_{(1)}), \quad c_{(2)} = a_{(1)}^2 + a_{(1)}b_{(1)} + b_{(1)}^2 - a_{(2)} - b_{(2)} + v_{(1)}w_{(1)}. \quad (39)$$

4. Asymptotic expansion of the constitutive relations

On computing the expansion of the eigenvalues of \mathbf{F} from Eq. (36) and hence of \mathcal{J}_1 , and simplifying using Eqs. (39), we obtain

$$\begin{aligned} \mathcal{J}_1 &= 3 + \varepsilon [2(a_{(1)} + b_{(1)} + c_{(1)})] + \varepsilon^2 [a_{(1)}^2 + b_{(1)}^2 + c_{(1)}^2 + v_{(1)}^2 + w_{(1)}^2 + 2(a_{(2)} + b_{(2)} + c_{(2)})] + O(\varepsilon^3) \\ &= 3 + \varepsilon^2 [4(a_{(1)}^2 + a_{(1)}b_{(1)} + b_{(1)}^2)] + O(\varepsilon^3). \end{aligned} \quad (40a)$$

Hence, from Eqs. (37) and on introducing $x = \lambda_s^0 Z^0$ and $\Lambda_s = L_s/\lambda_s^0$, $\Lambda_\phi = L_\phi/\lambda_s^0$,

$$\begin{aligned} \mathcal{J}_1 &= 3 + \frac{\varepsilon^2}{(1-x)^4} \left\{ [1 + (1-x)^2]^2 E_s^2 + 2[1 + (1-x)^2] E_s E_\phi + (4 - 12x + 18x^2 - 12x^3 + 3x^4) E_\phi^2 \right. \\ &\quad - 2x(4 - 6x + 4x^2 - x^3) E_s \Lambda_s - 2x(2 - x) E_\phi \Lambda_s - \frac{2x}{3} (6 - 12x + 11x^2 - 5x^3 + x^4) E_s \Lambda_\phi \\ &\quad - \frac{2x}{3} (12 - 39x + 55x^2 - 36x^3 + 9x^4) E_\phi \Lambda_\phi + x^2(2 - x)^2 \Lambda_s^2 + \frac{2x^2}{3} (6 - 9x + 5x^2 - x^3) \Lambda_s \Lambda_\phi \\ &\quad \left. + \frac{x^2}{9} (36 - 126x + 177x^2 - 114x^3 + 28x^4) \Lambda_\phi^2 \right\} + O(\varepsilon^3). \end{aligned} \quad (40b)$$

This determines the leading-order term of the asymptotic expansion of the energy density in Eq. (18). On defining, from Eq. (36), the (symmetric) effective two-dimensional deformation gradient and associated two-dimensional strain tensor,

$$\hat{\mathbf{F}} = \begin{pmatrix} 1 + \varepsilon a_{(1)} & 0 \\ 0 & 1 + \varepsilon b_{(1)} \end{pmatrix} + O(\varepsilon^2), \quad \hat{\mathbf{e}} = \frac{\hat{\mathbf{F}}^\top \hat{\mathbf{F}} - \mathbf{I}}{2}, \quad (41)$$

wherein \mathbf{I} is the identity, we rewrite Eq. (40a) as

$$\mathcal{J}_1 - 3 = 2 \left[(\text{tr } \hat{\mathbf{e}})^2 + \text{tr } (\hat{\mathbf{e}}^2) \right] + O(\varepsilon^3). \quad (42)$$

This shows how, at leading order, the energy density depends only on the two invariants of the effective two-dimensional strain tensor. In the asymptotic limit of a thin shell, the constitutive relations have thus become effectively two-dimensional.

5. Intrinsic volume conservation

To complete the derivation of the shell energy, we must specify the intrinsic deformations, and in particular how ζ^0 and hence Z^0 depend on ζ . Volume conservation between the undeformed and intrinsic configurations of the shell requires equality of the corresponding volume elements, $dV = dV^0$, which condition becomes

$$\begin{aligned} f_s^0 f_\phi^0 (1 - \varepsilon \kappa_s^0 \zeta^0) (1 - \varepsilon \kappa_\phi^0 \zeta^0) r \, ds \, d\phi \, d\zeta^0 \\ = (1 - \varepsilon \kappa_s \zeta) (1 - \varepsilon \kappa_\phi \zeta) r \, ds \, d\phi \, d\zeta, \end{aligned} \quad (43)$$

This, on recalling that $\kappa_s^0 = O(\varepsilon^{-1})$ yields, at leading order, a differential equation for $Z^0(\zeta)$,

$$(1 - \lambda_s^0 Z^0) Z_{,\zeta}^0 = 1 \implies Z^0 = \frac{1}{\lambda_s^0} \left(1 - \sqrt{1 - 2\lambda_s^0 \zeta} \right), \quad (44)$$

on imposing $Z^0 = 0$ at $\zeta = 0$. The shell surfaces are at $\zeta^0 = \pm h^0/2$ in the intrinsic configuration, and at $\zeta = \pm h_{\pm}$ in the undeformed configuration, where $h_+ + h_- = h$ is the undeformed thickness of the cell sheet. Let $H^0 = h^0 f_s^0 f_\phi^0$. Eq. (44) yields

$$h_{\pm} = \frac{H^0}{2} \left(1 \mp \frac{\lambda_s^0}{4} H^0 \right) \implies h = h_+ + h_- = H^0. \quad (45)$$

Finally, we introduce $\eta = \lambda_s^0 h$, so that the shell surfaces are at $x = \pm\eta/2$. We note that Eq. (45) is a leading-order result only, since we have ignored $O(\varepsilon)$ corrections in Eq. (44).

6. Derivation of the thin shell theory

We are now set up to average out the transverse coordinate and thus obtain the thin shell theory. We note, from Eq. (43), the expression for the volume element in the intrinsic configuration,

$$\begin{aligned} dV^0 &= \varepsilon(1 - \lambda_s^0 Z^0) r \, ds \, d\phi \, dZ^0 + O(\varepsilon^2) \\ &= \frac{1-x}{\lambda_s^0} \varepsilon r \, ds \, d\phi \, dx + O(\varepsilon^2). \end{aligned} \quad (46)$$

On substituting Eqs. (40b) and (46) into Eq. (18), integrating with respect to x , and using axisymmetry, we obtain

$$\mathcal{E} = \int_{\mathcal{S}} \hat{e} r \, ds \, d\phi = 2\pi \int_{\mathcal{C}} \hat{e} r \, ds, \quad (47a)$$

with the first integration over the undeformed axisymmetric midsurface \mathcal{S} and the second over the curve \mathcal{C} generating \mathcal{S} . The effective two-dimensional energy density \hat{e} in Eq. (47a) is

$$\begin{aligned} \hat{e} &= \frac{\varepsilon}{\lambda_s^0} \int_{-\eta/2}^{\eta/2} e(x)(1-x) \, dx = \frac{C}{2} \varepsilon^3 \left\{ h [\alpha_{ss} E_s^2 + (\alpha_{s\phi} + \alpha_{\phi s}) E_s E_\phi + \alpha_{\phi\phi} E_\phi^2] + 2h^2 [\beta_{ss} E_s L_s + \beta_{s\phi} E_s L_\phi + \beta_{\phi s} E_\phi L_s \right. \\ &\quad \left. + \beta_{\phi\phi} E_\phi L_\phi] + h^3 [\gamma_{ss} L_s^2 + (\gamma_{s\phi} + \gamma_{\phi s}) L_s L_\phi + \gamma_{\phi\phi} L_\phi^2] \right\} + O(\varepsilon^4), \end{aligned} \quad (47b)$$

wherein

$$\alpha_{ss} = \frac{\eta^4 - 8\eta^2 + 32}{(4 - \eta^2)^2} + \frac{4}{\eta} \tanh^{-1} \left(\frac{\eta}{2} \right), \quad (48a)$$

$$\alpha_{s\phi} = \alpha_{\phi s} = \frac{16}{(4 - \eta^2)^2} + \frac{2}{\eta} \tanh^{-1} \left(\frac{\eta}{2} \right), \quad (48b)$$

$$\alpha_{\phi\phi} = \frac{3\eta^4 - 24\eta^2 + 64}{(4 - \eta^2)^2}, \quad (48c)$$

$$\beta_{ss} = \frac{\eta^3 - 8\eta}{(4 - \eta^2)^2}, \quad (48d)$$

$$\beta_{s\phi} = \frac{\eta^6 + 16\eta^4 - 176\eta^2 + 192}{36\eta(4 - \eta^2)^2} - \frac{2}{3\eta^2} \tanh^{-1} \left(\frac{\eta}{2} \right), \quad (48e)$$

$$\beta_{\phi s} = -\frac{16}{\eta(4 - \eta^2)^2} + \frac{2}{\eta^2} \tanh^{-1} \left(\frac{\eta}{2} \right), \quad (48f)$$

$$\beta_{\phi\phi} = \frac{3\eta^5 - 20\eta^3 + 16\eta}{12(4 - \eta^2)^2}, \quad (48g)$$

$$\gamma_{ss} = \frac{\eta^4 - 8\eta^2 + 32}{\eta^2(4 - \eta^2)^2} - \frac{4}{\eta^3} \tanh^{-1} \left(\frac{\eta}{2} \right), \quad (48h)$$

$$\gamma_{s\phi} = \gamma_{\phi s} = \frac{\eta^6 - 8\eta^4 + 16\eta^2 + 192}{36\eta^2(4 - \eta^2)^2} - \frac{2}{3\eta^3} \tanh^{-1} \left(\frac{\eta}{2} \right), \quad (48i)$$

$$\gamma_{\phi\phi} = \frac{5\eta^4 - 42\eta^2 + 96}{18(4 - \eta^2)^2} \quad (48j)$$

are functions of

$$\eta = \lambda_s^0 h = \frac{\kappa_s^0}{f_s^0 f_\phi^0} (\varepsilon h) = \kappa_s^0 (\varepsilon h^0) \quad (49)$$

only. All of these coefficient functions diverge as $\eta \rightarrow \pm 2$; this divergence, absent from theories not valid for large bending deformations, is not surprising. Indeed, the limit $\eta \rightarrow \pm 2$ corresponds to constricted cells, i.e. wedge-shaped, triangular cells [Fig. 1(b), inset] for which the radius of curvature is half the intrinsic cell sheet thickness: either the apical or basal surface has become geometrically singular by contracting to a point. As the intrinsic configuration approaches this constricted limit somewhere, deviations from the intrinsic configuration become more and more expensive energetically there compared to other positions in the cell sheet. Fig. 3 makes a more general point by plotting the coefficient functions in Eqs. (48), arbitrarily scaled with α_{ss} to absorb their divergence as $\eta \rightarrow \pm 2$. This shows how the relative importance of different deformation modes depends on the amount of intrinsic bending. In other words, large bending deformations break the material isotropy, so that different directions of stretching have different effective stretching moduli; similarly, different effective bending moduli are associated with different directions of bending. This anisotropy is therefore geometric; as discussed in more detail below, this effect is absent from previous theories not valid for large bending deformations.

Moreover, rearranging Eqs. (22) and (23), the shell strains

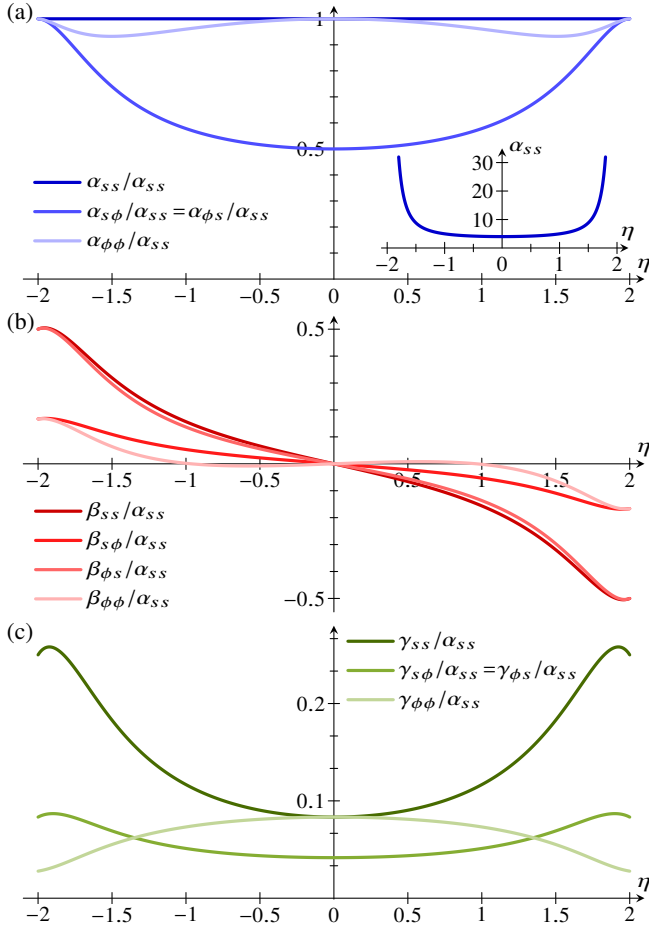


FIG. 3. Effective two-dimensional energy density. Plots of the coefficients defined in Eqs. (48) against η . All coefficients are arbitrarily scaled with α_{ss} to absorb their divergence in the constriction limit $\eta \rightarrow \pm 2$. (a) Plot of the stretching coefficients $\alpha_{ss}, \alpha_{s\phi}, \alpha_{\phi s}, \alpha_{\phi\phi}$. Inset: unscaled plot of α_{ss} against η , diverging as $\eta \rightarrow \pm 2$. (b) Plot of the mixed coefficients $\beta_{ss}, \beta_{s\phi}, \beta_{\phi s}, \beta_{\phi\phi}$. (c) Plot of the bending coefficients $\gamma_{ss}, \gamma_{s\phi}, \gamma_{\phi s}, \gamma_{\phi\phi}$.

in Eq. (47b) are

$$\varepsilon E_s = \frac{f_s - f_s^0}{f_s^0}, \quad \varepsilon E_\phi = \frac{f_\phi - f_\phi^0}{f_\phi^0}, \quad (50)$$

while the curvature strains are

$$L_s = \frac{\kappa_s - \kappa_s^0}{f_s^0 f_\phi^0} = K_s + O(\varepsilon), \quad L_\phi = \frac{\kappa_\phi - \kappa_\phi^0}{f_s^0 f_\phi^0} = K_\phi + O(\varepsilon), \quad (51a)$$

where we have defined

$$K_s = \frac{f_s \kappa_s - f_s^0 \kappa_s^0}{(f_s^0)^2 f_\phi^0}, \quad K_\phi = \frac{f_\phi \kappa_\phi - f_\phi^0 \kappa_\phi^0}{f_s^0 (f_\phi^0)^2}. \quad (51b)$$

At leading order (i.e. at the order to which the shell theory is valid), we may choose to replace the curvature strains L_s, L_ϕ in Eq. (47b) with the alternative curvature strains K_s, K_ϕ defined

above. The latter choice may be more natural since K_s, K_ϕ vanish for pure stretching deformations, whereas L_s, L_ϕ do not: consider a shell, the undeformed (and intrinsic) configuration of which is a sphere of radius R , and which deforms into a sphere of radius $R' = fR$, for example because of a pressure difference between the inside and outside. For this deformation, $f_s^0 = f_\phi^0 = 1$, $\kappa_s^0 = \kappa_\phi^0 = 1/R$, $f_s = f_\phi = f$, $\kappa_s = \kappa_\phi = 1/fR$, and so $L_s = L_\phi = (1 - f)/f^3 R \neq 0$ for $f \neq 1$, but $K_s = K_\phi = 0$. In other words, Eqs. (51a) show that the stretching deformations associated with changes in curvature can be neglected at leading order in the shell theory. Ref. [15] has also discussed this point.

This completes the derivation of the elastic energy (47a) of a thin shell undergoing large axisymmetric bending deformations. In Appendix B, we derive the governing equations associated with Eq. (47a). We solve these equations numerically using the boundary value problem solver `bvp4c` of MATLAB (The MathWorks, Inc.) and the continuation software `AUTO` [28].

C. Limit of small bending deformations

We conclude our calculations by taking the limit $\eta \rightarrow 0$, in which the bending deformations become small compared to the thickness of the shell. The energy density in Eq. (47b) then limits to the form familiar from classical shell theories,

$$\varepsilon \rightarrow 2C\varepsilon^3 \left[h \left(E_s^2 + E_s E_\phi + E_\phi^2 \right) + \frac{h^3}{12} \left(K_s^2 + K_s K_\phi + K_\phi^2 \right) \right], \quad (52)$$

up to corrections of order $O(\varepsilon^4)$. This is the energy density of a thin Hookean shell [15, 22, 23] with Poisson's ratio $\nu = 1/2$, implying incompressibility, and elastic modulus $E = 6C$. In particular, our analysis also provides a formal derivation of the morphoelastic version of this classical shell theory. The first term in the sum in square brackets is the stretching energy, while the second term is the bending energy. To pick up on a point made earlier, we note that, in this theory, the same stretching modulus $Eh/(1 - \nu^2) = 8Ch$ and the same bending modulus $Eh^3/[12(1 - \nu^2)] = 2Ch^3/3$ are associated with all directions of stretching or bending; it is this isotropy resulting from the constitutively assumed isotropy of the material that is broken by the geometry of large bending deformations.

Of course, Eq. (52) could be derived directly by imposing different scalings, of small intrinsic bending, replacing those for large bending deformations in Eq. (21); these scalings would considerably simplify the solutions of Eqs. (29), (30), and (34). Indeed, the structure of these calculations would be broadly similar to the earlier asymptotic derivation of the classical shell theories in Ref. [16]. We are not however aware of previous work pointing out, as we did above, that the terms at order $O(\varepsilon^2)$ in the expansion (36) of the deformation gradient need not be computed explicitly.

We note that Eq. (52) has the same structure as the elastic energies used in previous models referenced in the introduction, but the morphoelastic definitions of the shell and curvature strains in Eqs. (50) and (51b) differ from those in these previous models: in models not based on morphoelasticity

and its multiplicative decomposition of the deformation gradient [7, 8, 11–13], the shell and curvature strains are simply differences of stretches or curvatures, missing the scaling factors of f_s^0, f_ϕ^0 that appear in Eqs. (50) and (51b). We also note that the expressions for the curvature strains in Eqs. (51b) differ, by a factor of $f_s^0 f_\phi^0$, from those in Refs. [9, 10], which, as discussed earlier, derived morphoelastic shell theories based on a geometric approach. The geometric role of this factor has been noticed previously in the context of uniform growth of an elastic shell [29].

Moreover, the geometric approach in Refs. [9, 10] leads to additional terms in the energy density. The present analysis proves that these terms are not leading-order terms in the thin shell limit. However, there is no reason to expect this geometric approach to yield all terms at next order in the asymptotics. A complete expansion could in principle be obtained by continuing the asymptotic analysis presented here. This would permit asymptotic justification of the so-called shear deformation theories [30] in which the normals to the undeformed midsurface need not remain normals in the deformed configurations, but we do not pursue this further here.

III. INVAGINATION IN VOLVOX

A. Biological background

The green algal genus *Volvox* [31] has become a model for the study of the evolution of multicellularity [32, 33], for biological fluid dynamics [34], and for problems in developmental biology [35, 36]. Adult *Volvox* colonies [Fig. 4(a)] are spheroidal, consisting of several thousand biflagellated somatic cells that enclose a small number of germ cells [31]. Each germ cell undergoes several rounds of cell division to form a spherical embryonic cell sheet [Figs. 4(b) and 4(e)], at which stage those cell poles whence will emanate the flagella point into the sphere [31]. To acquire motility, the embryo turns itself inside out in a process called inversion [25, 37].

In some species of *Volvox* [25, 26], inversion starts with the formation of a circular invagination [Figs. 4(c) and 4(f)], reminiscent of the cell sheet folds associated with processes such as gastrulation or neurulation in higher organisms. At the cell level, this invagination results from two types of cell shape changes [7, 26]: (1) cells near the equator become wedge-shaped [Fig. 4(d)], while the cytoplasmic bridges (cell-cell connections resulting from incomplete division) rearrange to connect the cells at their thin wedge ends, and (2) cells in the posterior hemisphere narrow in the meridional direction. These cell shape changes arise simultaneously, with (1) splaying the cells and thereby bending the cell sheet [Fig. 4(d)] and (2) contracting the posterior hemisphere to facilitate the subsequent inversion of the posterior hemisphere inside the as yet uninverted anterior hemisphere. In later stages of inversion, other cell shape changes arise in different parts of the cell sheet [9, 26] to facilitate the peeling of the anterior hemisphere over the inverted posterior and thus complete inversion.

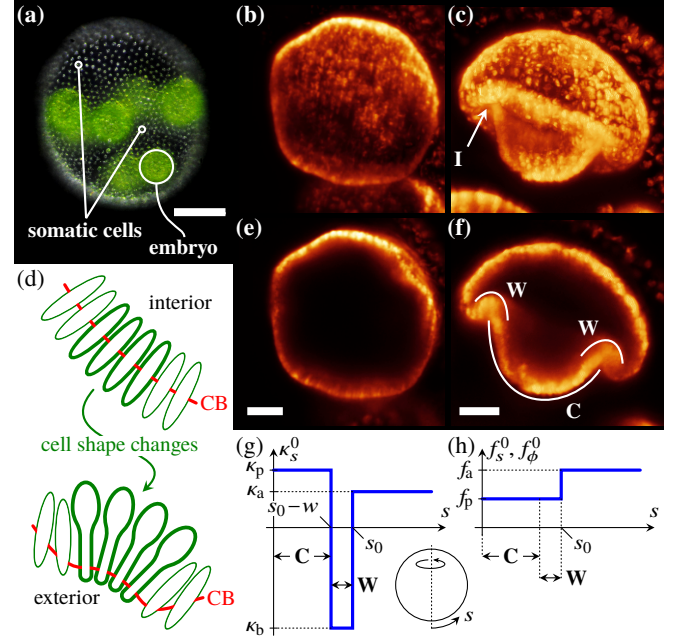


FIG. 4. Invagination in *Volvox*. (a) *Volvox* colony, with somatic cells and one embryo labelled. (b) Light-sheet microscopy image of a spherical *Volvox* embryo before inversion. (c) Corresponding image at an early stage of inversion, when a circular invagination (I) has formed. (d) Splaying of cells and bending of the cell sheet result from the formation of wedge-shaped cells and the rearrangement of the cytoplasmic bridges (CBs); red lines indicate position of CBs. (e) Midsagittal cross-section of a *Volvox* embryo before inversion. (f) Corresponding cross-section during invagination, with the regions where wedge-shaped cells (W) and contracted spindle-shaped cells (C) have formed labelled. (g) Plot of the intrinsic curvature κ_s^0 against arclength s , defined in the inset. The plot defines the model parameters $\kappa_p, \kappa_b, \kappa_a, s_0$, and w . Regions of cell shape changes (W, C) as in (f) are also indicated. (h) Corresponding plot of the intrinsic stretches f_s^0, f_ϕ^0 , defining additional model parameters f_p, f_a . Panels (a)–(f) include microscopy images by Stephanie Höhn and have been redrawn from Ref. [8]. Scale bars: (a) 50 μm ; (e), (f) 20 μm .

B. Results

Following our earlier work [7–10], we model *Volvox* inversion by considering the deformations of an incompressible elastic spherical shell under quasi-static axisymmetric variations of its intrinsic stretches and curvatures representing the cell shape changes driving inversion. The slow speed of inversion—it takes about an hour for a *Volvox* embryo to turn itself inside out [25, 26]—justifies this quasi-static approximation. In more detail, Figs. 4(g) and 4(h) show functional forms of the intrinsic stretches and curvatures encoding the cell shape changes driving invagination and define the model parameters $\kappa_p, \kappa_b, \kappa_a, f_p, f_a, s_0$, and w that encode the intrinsic curvatures and intrinsic stretches of different regions of the cell sheet and the extent of these regions. In numerical calculations, we regularise the step discontinuities in the definitions of the intrinsic stretches and curvatures in Figs. 4(g) and 4(h), we non-dimensionalise all lengths with the pre-inversion radius R of the embryo, and we take $\varepsilon h = 0.15$, appropriate for *Volvox globator* [7, 9].

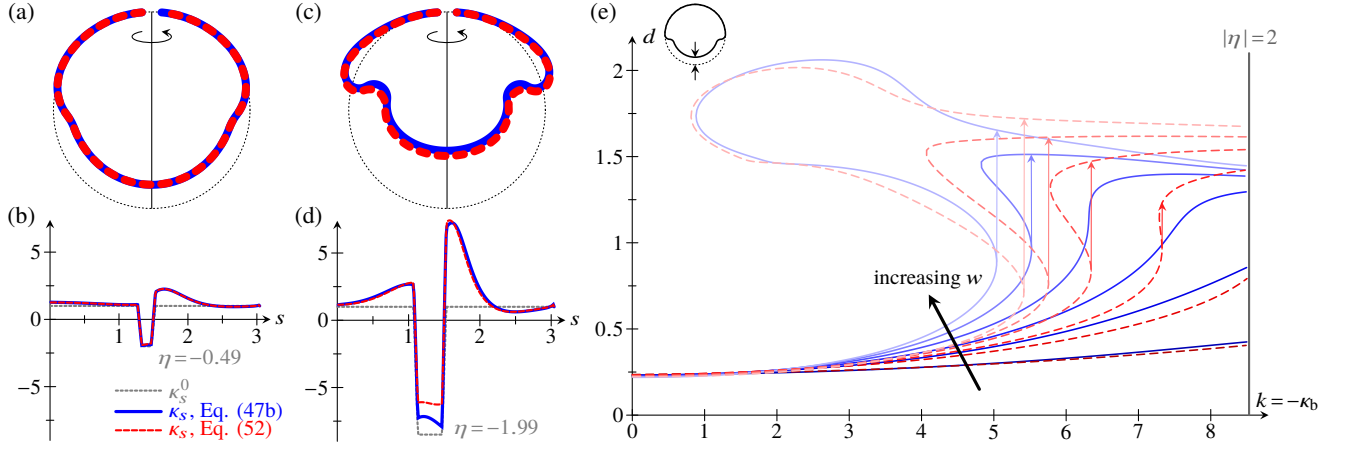


FIG. 5. Comparison of the elastic model for large bending deformations (solid lines), with energy density given by Eq. (47b), and the classical model (dashed lines), with energy density given by Eq. (52). (a) Early invagination stage: the two models yield very similar shapes. Dotted line: undeformed configuration of the spherical shell. Parameter values: $\kappa_p = \kappa_a = 1$, $\kappa_b = -2$, $f_p = 0.8$, $f_a = 1$, $s_0 = 1.5$, $w = 0.2$. (b) Corresponding plot of the meridional curvature and intrinsic curvature. (c) Later invagination stage: as the cells in the bend region approach the constriction limit, the shapes resulting from the two models start to differ. Parameter values are as in (a), except $\kappa_b = -8.5$, $w = 0.4$. (d) Corresponding plot of the meridional curvature and intrinsic curvature. (e) Bifurcation diagram, for different values of w , in (k, d) space, with $k = -\kappa_b$ and with d the posterior displacement defined in the axis inset. Different lines correspond to parameter values $w = 0.3, 0.5, 0.6, 0.7, 0.8, 0.9$. Other parameter values are as in (a). The vertical line $|\eta| = 2$ corresponding to the constriction limit is also shown. Vertical arrows indicate discontinuous jumps in d as k is increased.

During the invagination stage, the radius of curvature in the bend region of wedge-shaped cells [Fig. 4(f)] becomes comparable to the thickness of the cell sheet: this is the scaling limit of large bending deformations studied in Section II. We therefore compare the resulting elastic model, with energy density (47b), to the classical theory, in which the energy density is given by Eq. (52). For weakly invaginated stages of *Volvox* inversion (corresponding to small values of η in the large bending theory), the two models yield, unsurprisingly, very similar shapes [Fig. 5(a)], mirrored by very similar profiles of meridional curvature [Fig. 5(b)]. However, the more the intrinsic configuration of the cell sheet approaches the limit of cell constriction, the more the shapes resulting from the two models differ [Fig. 5(c)]. The curvature profile of these shapes differ in particular in the bend region of nearly constricted cells [Fig. 5(d)], as expected: since the coefficients defined in Eqs. (48) diverge in the constriction limit, deviations from the intrinsic configuration become increasingly expensive there in the large bending theory, but not in the classical theory. For this reason, the cell sheet is more invaginated in the large bending theory than in the classical theory [Fig. 5(c)]. In this way, the geometric effects of large bending stabilise the invagination process.

These examples indicate that the results of the two models differ at a quantitative, if not at a qualitative level. We extend this observation by plotting $k = -\kappa_b$ against the displacement d of the posterior pole [Fig. 5(e), inset] for different values of the width w of the bend region in Fig. 5(e). Again, the solution curves show similar behaviour in the two models, but differ at a quantitative level. There is a critical bend region width w_* such that the solution curves in the (k, d) diagram are single-valued for $w < w_*$, but become multivalued for $w > w_*$, leading to discontinuous jumps in d as k is varied. Where multiple solutions exist for a given value of k , the one

with the lowest value of d has the lowest energy (not shown). For the classical theory, we have discussed this bifurcation behaviour in Ref. [8], and rationalised it by constructing an effective energy that estimates different elastic contributions. It is therefore not surprising that, here, we find qualitatively identical bifurcation behaviour in the two models, but, again, there are quantitative differences in the bifurcation behaviour of the two theories. In particular, we note that w_* is larger in the large bending theory than in the classical theory. In other words, continuous invagination is possible in a larger region of parameter space in the large bending theory than in the classical theory, so, again, the geometry of large bending deformations is stabilising.

IV. CONCLUSION

In this paper, we have derived a morphoelastic shell theory valid for the large bending deformations that are commonly observed in developmental biology (Fig. 1), and have shown how this new scaling limit of large bending deformations induces a purely geometric effective material anisotropy absent from classical theories. Taking the invagination of the green alga *Volvox* as an example, we have compared this theory to a simpler, classical theory not formally valid for these large bending deformations. Since the classical theory does not account for the geometric singularity of cell constriction, it differs, for strongly invaginated shapes as in Figs. 1(b), 4(c), and 4(f), from the theory for large bending deformation at a quantitative, if not at a qualitative level. In particular, we have argued that this geometric limit stabilises invagination.

This and the growing interest in quantitative rather than merely qualitative analyses of morphogenesis [38, 39] emphasise the importance of this new scaling limit of large bending

deformations for studies of the mechanics of developmental biology. The theory we have derived here is not however the most general theory of these large bending deformations. Indeed, when writing down the expression for the intrinsic deformation gradient in Eq. (16), we assumed that there is no intrinsic displacement parallel to the midsurface, $\varsigma^0 = 0$. For $\varsigma^0 \neq 0$, we would replace the expansion of S posited in Eq. (27) with $S = S^0 + S_{(0)} + O(\varepsilon)$, where $S^0 = f_s^0 f_\phi^0 \varsigma^0$. The nonlinear differential equations extending Eqs. (29) and (30) that arise in the expansions of the boundary and incompressibility conditions in this more general case still admit a trivial solution $S_{(0)} \equiv 0$, $Z_{(0)} \equiv 0$, $p_{(0)} = 1$, but we were unable to extend our calculations in Section II to prove that this solution is unique; we raise a similar issue in Appendix C. It therefore remains unclear what form the extension of the Kirchhoff “hypothesis” [15] to this case takes.

In this paper, we assumed the simplest, incompressible Neo-Hookean constitutive relations when deriving our shell theory for large bending deformations. The restriction to incompressible elastic materials is justified by the biological context of our analysis, in which the models derived here describe sheets of fluid-filled cells that are therefore indeed incompressible to a first approximation. However, the bulk elastic response of biological materials such as brain tissue is not linear [40–42]. The restriction to linear Neo-Hookean relations may therefore appear to be a limitation of the analysis, but that turns out not to be the case: in the thin shell limit, general hyperelastic constitutive relations reduce to Neo-Hookean relations. This result has been established previously for thin plates [20, 43], and, in Appendix C, we (partially) extend it to the large bending deformations of thin shells considered here. In the context of shell theories, the problem of specifying the nonlinear constitutive relations of biological tissues does not therefore arise. However, we have recently shown that the continuum limit of a class of discrete models of cell sheets involves not only nonlinear elastic, but also nonlocal, nonelastic terms [44]. Moreover, adding the geometric singularity of apical constriction (corresponding to triangular cells in the underlying discrete model) as a constraint to the variational problem that arises in this continuum limit remains an important open problem [44], solving which may provide a regularisation of the singularity that arises in the theory derived here. Meanwhile, this suggests that the journey towards understanding the continuum mechanics of biological materials, on which we have taken another step with the present analysis of large bending deformations of thin elastic shells, will continue to abound with new problems in nonlinear mechanics.

ACKNOWLEDGMENTS

We thank M. Gomez for comments on the manuscript, and gratefully acknowledge support from the Engineering and Physical Sciences Research Council (Established Career Fellowship EP/M017982/1 to R.E.G.), the Wellcome Trust (Investigator Award 207510/Z/17/Z to R.E.G.), and Magdalene College, Cambridge (Neville Research Fellowship to P.A.H.).

APPENDIX A: NON-AXISYMMETRIC LARGE BENDING DEFORMATIONS OF AN ELASTIC SHELL

In this Appendix, we extend the calculations for axisymmetric deformations of an elastic shell in Section II to general, non-axisymmetric deformations.

1. Non-axisymmetric deformations of an elastic shell

As in Section II, we begin by deriving an expression for the deformation gradient tensors of an elastic shell of thickness εh , where ε is, again, a small asymptotic parameter that expresses the thinness of the shell.

a. Undeformed configuration of the shell

We parameterise the undeformed midsurface \mathcal{S} of the shell in terms of generalised, not necessarily orthogonal coordinates; we shall use Greek letters to denote these coordinates. Thus, if $\boldsymbol{\rho}$ is the position of a point on \mathcal{S} , the tangent vectors there are $\mathbf{e}_\alpha = \partial \boldsymbol{\rho} / \partial \alpha$. The metric g of the midsurface thus has components $g_{\alpha\beta} = \mathbf{e}_\alpha \cdot \mathbf{e}_\beta$, and we set $g = \det g$.

Next, we define a basis \mathcal{B} for the shell by adjoining the normal vector \mathbf{n} to this tangent basis. The Weingarten and Gauß equations [45]

$$\mathbf{n}_{,\alpha} = \kappa_\alpha^\beta \mathbf{e}_\beta, \quad \mathbf{e}_{\alpha,\beta} = -\kappa_{\alpha\beta} \mathbf{n} + \Gamma_{\alpha\beta}^\gamma \mathbf{e}_\gamma, \quad (\text{A1})$$

in which commata denote partial differentiation, express the derivatives of the normal and tangent vectors in terms of the curvature tensor $\kappa_{\alpha\beta} = \mathbf{e}_\alpha \cdot \mathbf{n}_{,\beta}$ and the Christoffel symbols associated with the metric of the midsurface [45].

The position of a point in the undeformed configuration \mathcal{V} of the shell is $\mathbf{r} = \boldsymbol{\rho} + \varepsilon \zeta \mathbf{n}$, where ζ denotes the transverse coordinate, as defined in Fig. 2(c). Hence

$$\mathbf{r}_{,\alpha} = \left(\delta_\alpha^\beta + \varepsilon \zeta \kappa_\alpha^\beta \right) \mathbf{e}_\beta, \quad \mathbf{r}_{,\zeta} = \varepsilon \mathbf{n}, \quad (\text{A2})$$

wherein we have used the Weingarten equation (A1), and where δ is the Kronecker delta. The metric tensor G of the undeformed configuration therefore has components

$$G_{\zeta\zeta} = \varepsilon^2, \quad G_{\alpha\zeta} = G_{\zeta\alpha} = 0, \quad G_{\alpha\beta} = \mathbf{r}_{,\alpha} \cdot \mathbf{r}_{,\beta}. \quad (\text{A3})$$

b. Deformed configuration of the shell

We take the same generalised coordinates to parameterise the deformed midsurface of the shell, and define the tangent vectors $\tilde{\mathbf{e}}_\alpha$ at a point $\tilde{\boldsymbol{\rho}}$ on its midsurface $\tilde{\mathcal{S}}$. The metric \tilde{g} of the midsurface has components $\tilde{g}_{\alpha\beta} = \tilde{\mathbf{e}}_\alpha \cdot \tilde{\mathbf{e}}_\beta$. We extend the tangent basis of the midsurface to a basis $\tilde{\mathcal{B}}$ for the deformed shell by adding the unit normal $\tilde{\mathbf{n}}$, and introduce the corresponding curvature tensor $\tilde{\kappa}_{\alpha\beta} = \tilde{\mathbf{e}}_\alpha \cdot \tilde{\mathbf{n}}_{,\beta}$. Extending the setup in Fig. 2(e) to non-axisymmetric deformations, the position of a point in the deformed configuration $\tilde{\mathcal{V}}$ of the shell is

$$\tilde{\mathbf{r}} = \tilde{\boldsymbol{\rho}} + \varepsilon (\tilde{\zeta} \tilde{\mathbf{n}} + \tilde{\zeta}^\alpha \tilde{\mathbf{e}}_\alpha), \quad (\text{A4})$$

where $\tilde{\zeta}$ and ζ^α are the transverse and parallel displacements of this point relative to the midsurface. In particular, for these non-axisymmetric deformations, the displacement parallel to the midsurface is no longer a scalar. Using the Weingarten and Gauß equations (A1), we find

$$\tilde{\mathbf{r}}_{,\alpha} = \left(\delta_\alpha^\beta + \varepsilon \tilde{\zeta} \tilde{\kappa}_\alpha^\beta + \varepsilon \tilde{\zeta}^\beta_{,\alpha} \right) \tilde{\mathbf{e}}_\beta + \varepsilon \left(\tilde{\zeta}_{,\alpha} - \tilde{\zeta}^\beta \tilde{\kappa}_{\alpha\beta} \right) \tilde{\mathbf{n}}, \quad (\text{A5a})$$

$$\tilde{\mathbf{r}}_{,\zeta} = \varepsilon \left(\tilde{\zeta}_{,\zeta} \tilde{\mathbf{n}} + \tilde{\zeta}^\alpha_{,\zeta} \tilde{\mathbf{e}}_\alpha \right), \quad (\text{A5b})$$

in which $\tilde{\zeta}^\beta_{,\alpha} = \tilde{\zeta}^\beta_{,\alpha} + \Gamma_{\alpha\gamma}^\beta \tilde{\zeta}^\gamma$ is a covariant derivative.

c. Intrinsic configuration of the shell

We define the intrinsic configuration of the shell by specifying the intrinsic basis \mathcal{B}^0 of the shell, containing the vectors \mathbf{E}_α , which we think of as the intrinsic tangent vectors, and a unit vector \mathbf{N} normal to these tangent vectors. The metric g^0 of the intrinsic midsurface has components $g^0_{\alpha\beta} = \mathbf{E}_\alpha \cdot \mathbf{E}_\beta$, and we write $g^0 = \det g^0$. Further, we define the (symmetric) intrinsic curvature tensor $\kappa^0_{\alpha\beta} = \mathbf{E}_\alpha \cdot \mathbf{N}_{,\beta}$, and the metric tensor G^0 of the intrinsic configuration. Denoting by ζ^0 the intrinsic transverse displacement, G^0 has, by analogy with Eqs. (A2) and (A3), components

$$G^0_{\zeta\zeta} = \varepsilon^2 \left(\zeta^0_{,\zeta} \right)^2, \quad G^0_{\alpha\zeta} = G^0_{\zeta\alpha} = 0, \quad (\text{A6a})$$

and

$$\begin{aligned} G^0_{\alpha\beta} &= \left(\delta_\alpha^\gamma + \varepsilon \zeta^0 \kappa^0_{\alpha\gamma} \right) \left(\delta_\beta^\delta + \varepsilon \zeta^0 \kappa^0_{\beta\delta} \right) \mathbf{E}_\gamma \cdot \mathbf{E}_\delta \\ &= g^0_{\alpha\gamma} \left(\delta_\gamma^\delta + \varepsilon \zeta^0 \kappa^0_{\gamma\delta} \right) \left(\delta_\beta^\delta + \varepsilon \zeta^0 \kappa^0_{\beta\delta} \right). \end{aligned} \quad (\text{A6b})$$

When writing down these expressions, we have assumed, as we did in Section II, that there is no intrinsic displacement parallel to the midsurface, $\zeta^{0\alpha} = 0$.

d. Calculation of the deformation gradient tensors

The deformation gradient tensor relating the undeformed and deformed configurations of the shell is $\tilde{\mathbf{F}} = \tilde{\mathbf{r}}_{,\alpha} \otimes \mathbf{r}^{\cdot\alpha}$ by definition. Now, from Eq. (A3), $G^{\zeta\zeta} = \varepsilon^{-2}$, $G^{\alpha\zeta} = G^{\zeta\alpha} = 0$, and hence

$$\mathbf{r}^{\cdot\alpha} = G^{\alpha\gamma} (g_{\gamma\beta} + \zeta \kappa_{\gamma\beta}) \mathbf{e}^\beta, \quad \mathbf{r}^{\cdot\zeta} = \varepsilon^{-1} \mathbf{n}. \quad (\text{A7})$$

It follows that

$$\begin{aligned} \tilde{\mathbf{F}} &= (\delta_\gamma^\alpha + \varepsilon \tilde{\zeta} \tilde{\kappa}_\gamma^\alpha + \varepsilon \tilde{\zeta}^\alpha_{,\gamma}) G^{\gamma\delta} (g_{\delta\beta} + \varepsilon \zeta \kappa_{\delta\beta}) \tilde{\mathbf{e}}_\alpha \otimes \mathbf{e}^\beta \\ &\quad + \varepsilon (\tilde{\zeta}_{,\alpha} - \tilde{\zeta}^\gamma \tilde{\kappa}_{\alpha\gamma}) G^{\alpha\gamma} (g_{\gamma\beta} + \varepsilon \zeta \kappa_{\gamma\beta}) \tilde{\mathbf{n}} \otimes \mathbf{e}^\beta \\ &\quad + \tilde{\zeta}^\alpha_{,\zeta} \tilde{\mathbf{e}}_\alpha \otimes \mathbf{n} + \tilde{\zeta}_{,\zeta} \tilde{\mathbf{n}} \otimes \mathbf{n}. \end{aligned} \quad (\text{A8a})$$

or, in block matrix notation,

$$\tilde{\mathbf{F}} = \begin{pmatrix} \tilde{\mathbf{A}}\mathbf{H} & \tilde{\zeta}_{,\zeta} \\ \tilde{\mathbf{b}}^\top \mathbf{H} & \tilde{\zeta}_{,\zeta} \end{pmatrix} [\tilde{\mathcal{B}} \otimes \mathcal{B}^*], \quad (\text{A8b})$$

in which the asterisk denotes a dual basis, and where we have introduced

$$H^\alpha_\beta = G^{\alpha\gamma} (g_{\gamma\beta} + \varepsilon \zeta \kappa_{\gamma\beta}), \quad (\text{A9})$$

and we write

$$\tilde{\mathbf{A}}^\alpha_\beta = \delta^\alpha_\beta + \varepsilon \tilde{\zeta} \tilde{\kappa}_\beta^\alpha + \varepsilon \tilde{\zeta}^\alpha_{,\beta}, \quad \tilde{\mathbf{b}}_\alpha = \varepsilon (\tilde{\zeta}_{,\alpha} - \tilde{\zeta}^\beta \tilde{\kappa}_{\alpha\beta}). \quad (\text{A10})$$

By analogy with Eqs. (A8), the intrinsic deformation gradient tensor is

$$\begin{aligned} \mathbf{F}^0 &= \left(\delta_\gamma^\alpha + \varepsilon \zeta^0 \kappa^0_{\gamma\alpha} \right) G^{\gamma\delta} (g_{\delta\beta} + \varepsilon \zeta \kappa_{\delta\beta}) \mathbf{E}_\alpha \otimes \mathbf{e}^\beta \\ &\quad + \varepsilon \zeta^0_{,\alpha} G^{\alpha\gamma} (g_{\gamma\beta} + \varepsilon \zeta \kappa_{\gamma\beta}) \mathbf{N} \otimes \mathbf{e}^\beta + \zeta^0_{,\zeta} \mathbf{N} \otimes \mathbf{n}, \end{aligned} \quad (\text{A11a})$$

or, in block matrix notation,

$$\mathbf{F}^0 = \begin{pmatrix} \mathbf{A}^0 \mathbf{H} & \mathbf{0} \\ \mathbf{b}^{0\top} \mathbf{H} & \zeta^0_{,\zeta} \end{pmatrix} [\mathcal{B}^0 \otimes \mathcal{B}^*], \quad (\text{A11b})$$

Here we have again assumed that there is no intrinsic displacement parallel to the midsurface, $\zeta^{0\alpha} = 0$, and we have introduced

$$\mathbf{A}^0_\alpha_\beta = \delta^\alpha_\beta + \varepsilon \zeta^0 \kappa^0_{\beta\alpha}, \quad \mathbf{b}^0_\alpha = \varepsilon \zeta^0_{,\alpha}. \quad (\text{A12})$$

On inverting the block-lower triangular matrix in Eq. (A11b), we find

$$(\mathbf{F}^0)^{-1} = \begin{pmatrix} \mathbf{H}^{-1} (\mathbf{A}^0)^{-1} & \mathbf{0} \\ -\frac{\mathbf{b}^{0\top} (\mathbf{A}^0)^{-1}}{\zeta^0_{,\zeta}} & \frac{1}{\zeta^0_{,\zeta}} \end{pmatrix} [\mathcal{B} \otimes (\mathcal{B}^0)^*]. \quad (\text{A13})$$

The elastic deformation gradient is $\mathbf{F} = \tilde{\mathbf{F}}(\mathbf{F}^0)^{-1}$. From Eqs. (A8b) and (A13), we obtain

$$\mathbf{F} = \begin{pmatrix} (\tilde{\mathbf{A}} - \tilde{\zeta}_{,\zeta^0} \mathbf{b}^{0\top}) (\mathbf{A}^0)^{-1} & \tilde{\zeta}_{,\zeta^0} \\ (\tilde{\mathbf{b}}^\top - \tilde{\zeta}_{,\zeta^0} \mathbf{b}^{0\top}) (\mathbf{A}^0)^{-1} & \tilde{\zeta}_{,\zeta^0} \end{pmatrix} [\tilde{\mathcal{B}} \otimes (\mathcal{B}^0)^*]. \quad (\text{A14a})$$

We replace $\tilde{\mathcal{B}}$ with an intermediate basis $\tilde{\mathcal{B}}^0$ by replacing the tangent vectors using the transformation $\tilde{\mathbf{e}}_\alpha = U^\beta_\alpha \tilde{\mathbf{E}}_\beta$. Then

$$\mathbf{F} = \begin{pmatrix} \mathbf{U} (\tilde{\mathbf{A}} - \tilde{\zeta}_{,\zeta^0} \mathbf{b}^{0\top}) (\mathbf{A}^0)^{-1} & \mathbf{U} \tilde{\zeta}_{,\zeta^0} \\ (\tilde{\mathbf{b}}^\top - \tilde{\zeta}_{,\zeta^0} \mathbf{b}^{0\top}) (\mathbf{A}^0)^{-1} & \tilde{\zeta}_{,\zeta^0} \end{pmatrix} [\tilde{\mathcal{B}}^0 \otimes (\mathcal{B}^0)^*], \quad (\text{A14b})$$

The bases $\tilde{\mathcal{B}}$ or $\tilde{\mathcal{B}}^0$ and \mathcal{B}^0 are not necessarily orthogonal or normalised, so the map that maps the first onto the second is not now in general a rotation, but we can work around this issue using the following observation: since the unit normals $\tilde{\mathbf{n}}$ and \mathbf{N} are orthogonal to $\tilde{\mathbf{E}}_\alpha$ and \mathbf{E}_α respectively, we can choose $\tilde{\mathbf{E}}_\alpha$ in such a way that $\tilde{\mathcal{B}}^0$ is a rotation of \mathcal{B}^0 , represented by a matrix \mathbf{R} . In particular, if (abusing notation) \mathbf{F} denotes

the matrix in Eq. (A14b), then the deformation gradient is represented, with respect to $\mathcal{B}^0 \otimes (\mathcal{B}^0)^*$, by the matrix $\mathbf{R}\mathbf{F}$.

Further $\tilde{\mathbf{E}}_\alpha \cdot \tilde{\mathbf{E}}_\beta = \mathbf{E}_\alpha \cdot \mathbf{E}_\beta$ since rotations preserve distances and angles. Hence, on recalling the definitions of the metrics $\tilde{g}_{\alpha\beta}$ and $g^0_{\alpha\beta}$ of the deformed and intrinsic midsurfaces of the shell,

$$\begin{aligned}\tilde{g}_{\alpha\beta} &= \tilde{\mathbf{e}}_\alpha \cdot \tilde{\mathbf{e}}_\beta = U^\gamma_\alpha U^\delta_\beta \tilde{\mathbf{E}}_\gamma \cdot \tilde{\mathbf{E}}_\delta \\ &= U^\gamma_\alpha U^\delta_\beta \mathbf{E}_\gamma \cdot \mathbf{E}_\delta = U^\gamma_\alpha U^\delta_\beta g^0_{\gamma\delta}. \quad (\text{A15})\end{aligned}$$

2. Thin shell theory for large bending deformations

As in Section II, we assume that the shell is made of an incompressible neo-Hookean material, with energy given by Eq. (18). Given our above remark on modifying the bases, Eq. (19) still provides the expression for the (first) Piola–Kirchhoff stress tensor \mathbf{P} , now with respect to $\mathcal{B}^0 \otimes (\mathcal{B}^0)^*$: we still have $\mathbf{P} = \mathbf{R}\mathbf{Q}$, with $\mathbf{Q} = \mathbf{F} - p\mathbf{F}^{-\top}$, in which \mathbf{F} is now given by Eq. (A14b). Moreover, Eq. (20) still applies.

a. Scaling assumptions

Again as in Section II, we now introduce large bending deformations explicitly by scaling the intrinsic curvature tensor so as to absorb the intrinsic stretching of the midsurface,

$$\kappa^0_{\alpha\beta} = \sqrt{\frac{g^0}{g}} \frac{\lambda^0_{\alpha\beta}}{\varepsilon}. \quad (\text{A16})$$

Next, we make the standard scaling assumptions of shell theory, that the elastic strains remain small. First, we therefore require that the metrics \tilde{g} and g^0 be not “too different”. Introducing the shell strain tensor \mathbf{E} , and from Eq. (A15), we therefore impose

$$U^\alpha_\beta = \delta^\alpha_\beta + \varepsilon E^\alpha_\beta. \quad (\text{A17})$$

For axisymmetric deformations, these tensors are symmetric, and we recover the definition of the shell strains in Eq. (22). Similarly, we require the curvature tensors of the intrinsic and deformed configurations to be not “too different”. We therefore introduce the curvature strain tensor \mathbf{K} by writing

$$\tilde{\kappa}_{\alpha\beta} = \sqrt{\frac{g^0}{g}} \left(\frac{\lambda^0_{\alpha\beta}}{\varepsilon} + L_{\alpha\beta} \right), \quad (\text{A18})$$

Finally, we introduce scaled variables

$$Z^0 = \sqrt{\frac{g^0}{g}} \zeta^0, \quad Z = \sqrt{\frac{g^0}{g}} \tilde{\zeta}, \quad S = \sqrt{\frac{g^0}{g}} \tilde{\varsigma}. \quad (\text{A19})$$

b. Intrinsic volume conservation

We now impose volume conservation of the intrinsic configuration of the shell compared to the undeformed configuration. We need one preliminary result:

Lemma 1. Let \mathbf{M} be a 2×2 matrix, and x be a scalar. Then

$$\det(\mathbf{I} + x\mathbf{M}) = 1 + x \operatorname{tr} \mathbf{M} + x^2 \det \mathbf{M}.$$

Proof. By direct computation,

$$\begin{aligned}\det \begin{pmatrix} 1 + xM_{11} & xM_{12} \\ xM_{21} & 1 + xM_{22} \end{pmatrix} \\ = 1 + x(M_{11} + M_{22}) + x^2(M_{11}M_{22} - M_{12}M_{21}),\end{aligned}$$

which proves the claim. \square

Volume conservation between the undeformed and intrinsic configurations of the shell requires equality of the volume elements, $\sqrt{\det \mathbf{G}} = \sqrt{\det \mathbf{G}^0}$. Now, from Eqs. (A2) and (A3), $G_{\alpha\beta} = g_{\alpha\beta} + O(\varepsilon)$, and hence

$$\sqrt{\det \mathbf{G}} = \varepsilon \sqrt{g} + O(\varepsilon^2). \quad (\text{A20a})$$

Moreover, from Eqs. (A6) with the scalings introduced above and invoking Lemma 1, we find

$$\sqrt{\det \mathbf{G}^0} = \varepsilon \left(\sqrt{\frac{g}{g^0}} Z^0_{,\zeta} \right) \left\{ \sqrt{g^0} \left[1 + 2\mathcal{H}^0 Z^0 + \mathcal{K}^0 (Z^0)^2 \right] \right\}, \quad (\text{A20b})$$

wherein $\mathcal{H}^0 = \frac{1}{2} \operatorname{tr} \lambda^0$ and $\mathcal{K}^0 = \det \lambda^0$ are the (scaled) mean and Gaussian intrinsic curvatures [45]. The eigenvalues λ_1, λ_2 of λ^0 are real [45], and $\mathcal{H}^0 = \frac{1}{2}(\lambda_1 + \lambda_2)$, $\mathcal{K}^0 = \lambda_1 \lambda_2$, from which follows the well-known inequality $(\mathcal{H}^0)^2 \geq \mathcal{K}^0$.

Now, integrating the differential equation for $Z^0(\zeta)$ resulting from Eqs. (A20) and imposing $Z^0 = 0$ at $\zeta = 0$, we find

$$Z^0 + \mathcal{H}^0 (Z^0)^2 + \frac{\mathcal{K}^0}{3} (Z^0)^3 = \zeta. \quad (\text{A21})$$

Since Eq. (A20a) neglects $O(\varepsilon^2)$ corrections, this result holds at leading order only.

Now, as discussed in Section II, the shell surfaces are at $\zeta^0 = \pm h^0/2$ in the intrinsic configuration, and at $\zeta = \pm h_\pm$ in the undeformed configuration, where $h_+ + h_- = h$ is the undeformed thickness of the cell sheet. On defining $H^0 = h^0 \sqrt{g^0/g}$, so that the shell surfaces are at $Z^0 = \pm H^0/2$ in the intrinsic configuration, Eq. (A21) yields

$$h_\pm = \frac{H^0}{2} \left[1 \mp \frac{\mathcal{H}^0}{2} H^0 + \frac{\mathcal{K}^0}{12} (H^0)^2 \right], \quad (\text{A22a})$$

and hence

$$h = h_+ + h_- = H^0 + \frac{\mathcal{K}^0}{12} (H^0)^3, \quad (\text{A22b})$$

which is a depressed cubic equation for $H^0(h)$ that can be solved in closed form. In particular, Eq. (A22b) has a unique positive real solution if $\mathcal{K}^0 > 0$, but has no positive real solution if $h^2 \mathcal{K}^0 < -16/9$. If $0 > h^2 \mathcal{K}^0 > -16/9$, two positive real solutions exist; by continuity, the smaller must be chosen.

More generally, we require that ζ increases with Z^0 , for $|Z^0| \leq H^0/2$. As $(\mathcal{H}^0)^2 \geq \mathcal{K}^0$, the cubic in Eq. (A21) has

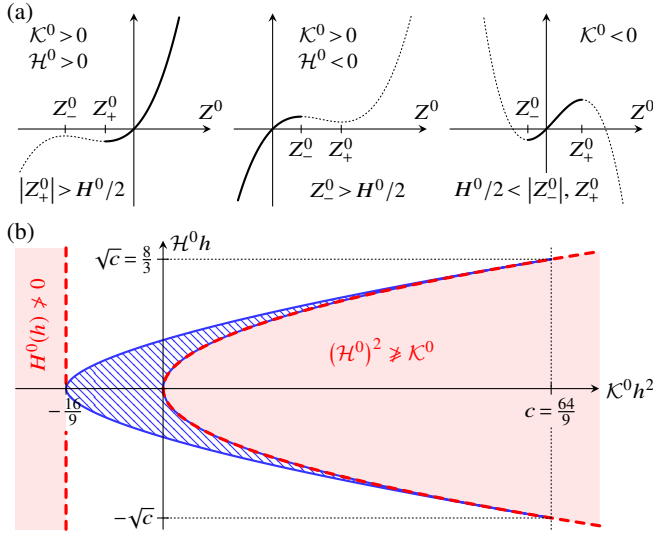


FIG. 6. Intrinsic volume conservation. (a) Plot of $\zeta(Z^0)$ defined in Eq. (A21) for the cases $\kappa^0 > 0, \mathcal{H}^0 > 0$; $\kappa^0 > 0, \mathcal{H}^0 < 0$; $\kappa^0 < 0$. The positions of the turning points at $Z^0 = Z_{\pm}^0$ are indicated, and $\zeta(Z^0)$ must increase monotonically for $|Z^0| < H^0/2$. This condition excludes the dotted parts of the graphs. (b) Intrinsic volume conservation in $(\kappa^0 h^2, \mathcal{H}^0 h)$ space: conservation of intrinsic volume is only possible within the region of parameter space enclosed by the solid curve, in which $-16/9 < h^2 \kappa^0 < c = 64/9$ and $h|\mathcal{H}^0| < \sqrt{c} = 8/3$. The dashed lines delimit the regions of parameter space excluded by the inequality $(\mathcal{H}^0)^2 \geq \kappa^0$ and the condition that Eq. (A22b) have a positive real solution.

two turning points [Fig. 6(a)], at $Z^0 = Z_{\pm}^0$, where explicit expressions for $Z_{\pm}^0 \leq Z_{\pm}^0$ in terms of κ^0, \mathcal{H}^0 can be found by solving a quadratic equation. The condition that ζ increases with Z^0 translates to inequalities $Z_{\pm}^0 \geq H^0(h)/2$ depending on the signs of κ^0, \mathcal{H}^0 [Fig. 6(a)]. These inequalities involving $h, \mathcal{H}^0, \kappa^0$ only depend on $\mathcal{H}^0 h$ and $\kappa^0 h^2$, since the curvatures can be nondimensionalised with h . The inequalities can then be solved numerically to determine the region in $(\kappa^0 h^2, \mathcal{H}^0 h)$ parameter space for which intrinsic volume conservation is possible [Fig. 6(b)]. In particular, Fig. 6(b) shows that intrinsic volume conservation requires $-16/9 \leq \kappa^0 h^2 \leq c$ and $|\mathcal{H}^0 h| \leq \sqrt{c}$, where c is a numerical constant. We note that an expression for the boundary of this region can also be determined in closed form using MATHEMATICA (Wolfram, Inc.); although rather complicated, this expression can be used to show that $c = 64/9$.

Finally, to relate this discussion to the results of Section II, we note that if $\kappa^0 = 0$, the condition is $|\mathcal{H}^0| \leq 1$, which is equivalent to $|\eta| \leq 2$, as expected.

c. Boundary conditions and condition of incompressibility

As in Section II, the incompressibility and boundary conditions read $\det F = 1$ and $Q^{\pm} N_{\pm} = \mathbf{0}$.

To derive an expression for the normals N_{\pm} , we compute the tangent vectors E_{α}^{\pm} to the surfaces of the intrinsic configuration of the shell, at $\zeta^0 = \pm h^0/2 \iff Z^0 = \pm H^0/2$. By analogy

with Eq. (A5a) and using the scalings in Eqs. (A16) and (A19),

$$E_{\alpha}^{\pm} = \left(\delta_{\alpha}^{\beta} \pm H^0 \lambda^0_{\alpha}{}^{\beta} / 2 \right) E_{\beta} \pm \left(\varepsilon h^0_{,\alpha} / 2 \right) N. \quad (\text{A23})$$

We now order $\mathcal{B}^0 = \{E_1, E_2, N\}$ so that $E_1 \times E_2 = \sqrt{g^0} N$, and hence $E_1 \times N = -E^2$, $E_2 \times N = E^1$. By expanding in components, we find

$$\begin{aligned} E_1^{\pm} \times E_2^{\pm} &= \left[1 \pm H^0 \mathcal{H}^0 + \frac{1}{4} (H^0)^2 \kappa^0 \right] \sqrt{g^0} N \\ &\mp \frac{1}{2} \varepsilon h^0_{,\alpha} \left[\left(1 \pm H^0 \mathcal{H}^0 \right) \delta^{\alpha}_{\beta} \mp \frac{1}{2} \lambda^0_{\beta}{}^{\alpha} H^0 \right] E^{\beta}. \end{aligned} \quad (\text{A24})$$

On normalising this vector, we deduce

$$N_{\pm} = \pm N - \varepsilon \frac{h^0_{,\alpha} \left[2 \left(1 \pm H^0 \mathcal{H}^0 \right) \delta^{\alpha}_{\beta} \mp H^0 \lambda^0_{\beta}{}^{\alpha} \right]}{\sqrt{g^0} \left[4 \left(1 \pm \mathcal{H}^0 H^0 \right) + (H^0)^2 \kappa^0 \right]} E^{\beta} + O(\varepsilon^2). \quad (\text{A25})$$

d. Expansion of the boundary and incompressibility conditions

To expand the boundary and incompressibility conditions, we extend Eqs. (27) by writing

$$Z = Z^0 + Z_{(0)} + \varepsilon Z_{(1)} + O(\varepsilon^2), \quad S = S_{(0)} + O(\varepsilon). \quad (\text{A26})$$

Solution at order $O(1)$. From Eqs. (A10) and (A12), and using the definitions (A19), we obtain the leading-order expansions

$$A^0_{\alpha}{}^{\beta} = \delta^{\alpha}_{\beta} + Z^0 \lambda^0_{\beta}{}^{\alpha}, \quad \tilde{A}^{\alpha}_{\beta} = A^0_{\beta}{}^{\alpha} + Z_{(0)} \lambda^0_{\beta}{}^{\alpha} + O(\varepsilon), \quad (\text{A27a})$$

and

$$b^0_{\alpha} = O(\varepsilon), \quad \tilde{b}_{\alpha} = -S_{(0)}^{\beta} \lambda^0_{\alpha\beta} + O(\varepsilon), \quad (\text{A27b})$$

and thence, from Eq. (A14b),

$$F = \left(\frac{B}{w^{\top}} \middle| \frac{v}{c} \right) + O(\varepsilon), \quad (\text{A28a})$$

in which dashes now denote differentiation with respect to Z^0 , and where, writing $\tilde{A} = \tilde{A}_{(0)} + O(\varepsilon)$, with $\tilde{A}_{(0)}$ given by Eq. (A27a),

$$B = \tilde{A}_{(0)} (A^0)^{-1}, \quad v = S'_{(0)}, \quad w = -(A^0)^{-\top} \lambda^0 S_{(0)}, \quad c = 1 + Z'_{(0)}. \quad (\text{A28b})$$

On computing the determinant of the block matrix [46] in Eq. (A28a), the incompressibility condition becomes

$$1 = \det F = (\det B) \left(c - w^{\top} B^{-1} v \right) + O(\varepsilon). \quad (\text{A29})$$

Using further properties of block matrices [46] and from Eq. (A28a), we obtain

$$F^{-\top} = \left(\begin{array}{c|c} O(1) & -B^{-\top} w (c - w^{\top} B^{-1} v)^{-1} \\ \hline O(1) & (c - w^{\top} B^{-1} v)^{-1} \end{array} \right) + O(\varepsilon), \quad (\text{A30})$$

and thus, writing $\mathbf{Q} = \mathbf{Q}_{(0)} + \varepsilon \mathbf{Q}_{(1)} + O(\varepsilon^2)$, $p = p_{(0)} + O(\varepsilon)$,

$$\mathbf{Q}_{(0)} \mathbf{N} = \left(\frac{\mathbf{v} + p_{(0)} \mathbf{B}^{-\top} \mathbf{w} (c - \mathbf{w}^\top \mathbf{B}^{-1} \mathbf{v})^{-1}}{c - p_{(0)} (c - \mathbf{w}^\top \mathbf{B}^{-1} \mathbf{v})^{-1}} \right). \quad (\text{A31})$$

Now, as in Section II, the governing equation (20) of three-dimensional elasticity is, at leading order, $(\mathbf{Q}_{(0)} \mathbf{N})_{,Z^0} = \mathbf{0}$. Using Eq. (A25), it follows that the boundary conditions read $\mathbf{0} = \mathbf{Q}^\pm \mathbf{N}_\pm = \mathbf{Q}_{(0)} \mathbf{N} + O(\varepsilon)$. Hence $\mathbf{Q}_{(0)} \mathbf{N} \equiv \mathbf{0}$ as in Section II.

From Eqs. (A28b), $\mathbf{w}^\top \mathbf{B}^{-1} = \mathbf{S}_{(0)}^\top \mathbf{D}$ with $\mathbf{D} = -(\lambda^0)^\top \tilde{\mathbf{A}}_{(0)}^{-1}$, so that $\mathbf{B}^{-\top} \mathbf{w} = \mathbf{D}^\top \mathbf{S}_{(0)}$. Eqs. (A29) and (A31) then yield the leading-order incompressibility and boundary conditions,

$$1 + Z'_{(0)} - \mathbf{S}_{(0)}^\top \mathbf{D} \mathbf{S}'_{(0)} = (\det \mathbf{B})^{-1}, \quad (\text{A32a})$$

and hence

$$\mathbf{S}'_{(0)} + p_{(0)} (\det \mathbf{B}) \mathbf{D}^\top \mathbf{S}_{(0)} = \mathbf{0}, \quad 1 + Z'_{(0)} - p_{(0)} (\det \mathbf{B}) = 0. \quad (\text{A32b})$$

In particular, noting that $\mathbf{S}'_{(0)} \mathbf{D}^\top \mathbf{S}_{(0)} = \mathbf{S}_{(0)}^\top \mathbf{D} \mathbf{S}'_{(0)}$ since this expression is a scalar,

$$\begin{aligned} \mathbf{S}'_{(0)} \mathbf{S}'_{(0)} &= -p_{(0)} (\det \mathbf{B}) \mathbf{S}'_{(0)} \mathbf{D}^\top \mathbf{S}_{(0)} = -p_{(0)} (\det \mathbf{B}) \mathbf{S}_{(0)}^\top \mathbf{D} \mathbf{S}'_{(0)} \\ &= -p_{(0)} (\det \mathbf{B}) [1 + Z'_{(0)} - (\det \mathbf{B})^{-1}] \\ &= p_{(0)} - (1 + Z'_{(0)})^2. \end{aligned} \quad (\text{A33})$$

Moreover, from Eqs. (A27) and the definition (A28b) and using Lemma 1, we obtain

$$\det \mathbf{B} = \frac{\det \tilde{\mathbf{A}}_{(0)}}{\det \mathbf{A}^0} = \frac{1 + 2\mathcal{H}^0 (Z^0 + Z_{(0)}) + \mathcal{K}^0 (Z^0 + Z_{(0)})^2}{1 + 2\mathcal{H}^0 Z^0 + \mathcal{K}^0 (Z^0)^2}. \quad (\text{A34})$$

Substituting in the second of Eqs. (A32b) and integrating,

$$\tanh^{-1} \frac{\mathcal{H}^0 + \mathcal{K}^0 (Z^0 + Z_{(0)})}{\sqrt{(\mathcal{H}^0)^2 - \mathcal{K}^0}} = p_{(0)} \tanh^{-1} \frac{\mathcal{H}^0 + \mathcal{K}^0 Z^0}{\sqrt{(\mathcal{H}^0)^2 - \mathcal{K}^0}} + a, \quad (\text{A35})$$

in which a is a constant of integration; the singular cases $\mathcal{K}^0 = 0$, $\mathcal{K}^0 = \mathcal{H}^0 = 0$, or $\mathcal{K}^0 = (\mathcal{H}^0)^2$ can be dealt with similarly, but we will not discuss these in detail.

Now, by definition, on the midsurface $Z^0 = 0$, we have $Z_{(0)} = 0$ and $\mathbf{S}_{(0)} = \mathbf{0}$. Thus $\det \mathbf{B} = 1$ on $Z^0 = 0$, and hence, successively from Eqs. (A32), $Z'_{(0)} = 0$, $\mathbf{S}'_{(0)} = \mathbf{0}$ on $Z^0 = 0$, and hence $p_{(0)} = 1$ (which is constant). Then taking $Z^0 = Z_{(0)} = 0$ in Eq. (A35) yields $a = 0$; the same equation then immediately yields $Z_{(0)} \equiv 0$. Finally, Eq. (A33) yields $\mathbf{S}'_{(0)} \mathbf{S}'_{(0)} = 0$, so $\mathbf{S}'_{(0)} \equiv \mathbf{0}$, and hence, since $\mathbf{S}_{(0)} = \mathbf{0}$ on $Z^0 = 0$, we find $\mathbf{S}_{(0)} \equiv \mathbf{0}$. This proves the Kirchhoff ‘‘hypothesis’’ [15] for general large bending deformations.

We note that, in the case of axisymmetric deformations, this argument provides an alternative to the direct integration of the leading-order equations in Section II.

Solution at orders $O(\varepsilon)$ and $O(\varepsilon^2)$. We now expand further. In particular, extending Eqs. (A27), we find

$$\tilde{\mathbf{A}} = \mathbf{A}^0 + \varepsilon (Z^0 \mathbf{L} + Z_{(1)} \lambda^0) + O(\varepsilon^2), \quad (\text{A36})$$

while now $\mathbf{b}^0, \tilde{\mathbf{b}}, \tilde{\boldsymbol{\zeta}} = O(\varepsilon)$, and hence

$$\mathbf{F} = \mathbf{I} + \varepsilon \left(\frac{\mathbf{E} + (Z^0 \mathbf{L} + Z_{(1)} \lambda^0) (\mathbf{A}^0)^{-1}}{O(1)} \middle| \frac{O(1)}{Z'_{(1)}} \right) + O(\varepsilon^2). \quad (\text{A37})$$

from Eq. (A14b), using Eq. (A17). Thus, using Lemma 1,

$$\det \mathbf{F} = 1 + \varepsilon \left\{ Z'_{(1)} + \text{tr} \mathbf{E} + \text{tr} \left[(Z^0 \mathbf{L} + Z_{(1)} \lambda^0) (\mathbf{A}^0)^{-1} \right] \right\} + O(\varepsilon^2). \quad (\text{A38})$$

The incompressibility condition $\det \mathbf{F} = 1$ thus yields, at order $O(\varepsilon)$, an ordinary differential equation for $Z_{(1)}$. To make further progress, we shall need the following result:

Lemma 2. *Let \mathbf{M} be a 2×2 matrix, and x be a scalar. Then*

$$(\mathbf{I} + x\mathbf{M})^{-1} = \frac{\mathbf{I} + x \text{adj } \mathbf{M}}{1 + x \text{tr } \mathbf{M} + x^2 \det \mathbf{M}}.$$

Proof. By definition of the adjugate matrix,

$$(\mathbf{I} + x\mathbf{M})^{-1} = \frac{\text{adj } (\mathbf{I} + x\mathbf{M})}{\det (\mathbf{I} + x\mathbf{M})} = \frac{\text{adj } (\mathbf{I} + x\mathbf{M})}{1 + x \text{tr } \mathbf{M} + x^2 \det \mathbf{M}},$$

using Lemma 1. But, by direct computation,

$$\begin{aligned} \text{adj } (\mathbf{I} + x\mathbf{M}) &= \begin{pmatrix} 1 + xM_{22} & -M_{12} \\ -M_{21} & 1 + xM_{22} \end{pmatrix} \\ &= \begin{pmatrix} 1 & 0 \\ 0 & 1 \end{pmatrix} + x \begin{pmatrix} M_{22} & -M_{12} \\ -M_{21} & M_{11} \end{pmatrix} = \mathbf{I} + x \text{adj } \mathbf{M}. \end{aligned}$$

The result follows. \square

On multiplying this result by a general 2×2 matrix \mathbf{N} and taking the trace on both sides, we obtain

Corollary 1. *Let \mathbf{M}, \mathbf{N} be 2×2 matrices, and let x be a scalar. The following equality holds:*

$$\text{tr} [\mathbf{N}(\mathbf{I} + x\mathbf{M})^{-1}] = \frac{\text{tr } \mathbf{N} + x \text{tr} (\mathbf{N} \text{adj } \mathbf{M})}{1 + x \text{tr } \mathbf{M} + x^2 \det \mathbf{M}}.$$

We shall also need the following observation:

Lemma 3. *Let \mathbf{M}, \mathbf{N} be 2×2 matrices. Then*

$$\text{tr} (\mathbf{N} \text{adj } \mathbf{M}) = \text{tr } \mathbf{M} \text{tr } \mathbf{N} - \text{tr} (\mathbf{M}\mathbf{N}) \text{ and } \text{tr} (\mathbf{M} \text{adj } \mathbf{M}) = 2 \det \mathbf{M}.$$

Proof. Notice that $\mathbf{M} + \text{adj } \mathbf{M} = (\text{tr } \mathbf{M})\mathbf{I}$ since

$$\begin{pmatrix} M_{11} & M_{12} \\ M_{21} & M_{22} \end{pmatrix} + \begin{pmatrix} M_{22} & -M_{12} \\ -M_{21} & M_{11} \end{pmatrix} = (M_{11} + M_{22}) \begin{pmatrix} 1 & 0 \\ 0 & 1 \end{pmatrix}.$$

Hence $\mathbf{N}\mathbf{M} + \mathbf{N} \text{adj } \mathbf{M} = (\text{tr } \mathbf{M})\mathbf{N}$ on multiplication by \mathbf{N} . Taking the trace gives the first result. The second result follows from the definition of the adjugate, $\mathbf{M} \text{adj } \mathbf{M} = (\det \mathbf{M})\mathbf{I}$, by taking the trace and noting that $\text{tr } \mathbf{I} = 2$. \square

Combining Corollary 1 and Lemma 3, and recalling the definitions $\text{tr } \lambda^0 = 2\mathcal{H}^0$, $\det \lambda^0 = \mathcal{K}^0$, the differential equation for $Z_{(1)}$ resulting from Eq. (A38) is

$$Z'_{(1)} + \left(\frac{2\mathcal{H}^0 + 2\mathcal{K}^0 Z^0}{1 + 2\mathcal{H}^0 Z^0 + \mathcal{K}^0 (Z^0)^2} \right) Z_{(1)} + \text{tr } \mathbf{E} + \frac{Z^0 \text{tr } \mathbf{L} + (Z^0)^2 [2\mathcal{H}^0 \text{tr } \mathbf{L} - \text{tr } (\mathbf{L}\lambda^0)]}{1 + 2\mathcal{H}^0 Z^0 + \mathcal{K}^0 (Z^0)^2} = 0. \quad (\text{A39})$$

Integrating and imposing $Z_{(1)} = 0$ at $Z^0 = 0$, we find

$$Z_{(1)} = - \frac{\left[Z^0 + \mathcal{H}^0 (Z^0)^2 + \frac{1}{3} \mathcal{K}^0 (Z^0)^3 \right] \text{tr } \mathbf{E} + \frac{1}{2} (Z^0)^2 \text{tr } \mathbf{L} + \frac{1}{3} (Z^0)^3 [2\mathcal{H}^0 \text{tr } \mathbf{L} - \text{tr } (\mathbf{L}\lambda^0)]}{1 + 2\mathcal{H}^0 Z^0 + \mathcal{K}^0 (Z^0)^2}. \quad (\text{A40})$$

Next, from Eq. (A37), we may write

$$\mathbf{F} = \left(\begin{array}{c|c} 1 + \varepsilon \mathbf{B}_{(1)} + \varepsilon^2 \mathbf{B}_{(2)} + O(\varepsilon^3) & \varepsilon \mathbf{v}_{(1)} + O(\varepsilon^2) \\ \hline \varepsilon \mathbf{w}_{(1)}^\top + O(\varepsilon^2) & 1 + \varepsilon c_{(1)} + \varepsilon^2 c_{(2)} + O(\varepsilon^3) \end{array} \right), \quad (\text{A41})$$

with, using Lemma 2,

$$\mathbf{B}_{(1)} = \mathbf{E} + \frac{(Z^0 \mathbf{L} + Z_{(1)} \lambda^0) (\mathbf{I} + Z^0 \text{adj } \lambda^0)}{1 + 2\mathcal{H}^0 Z^0 + \mathcal{K}^0 (Z^0)^2}, \quad (\text{A42})$$

in which $Z_{(1)}$ is given by Eq. (A40), and where explicit expressions for $\mathbf{B}_{(2)}$, $\mathbf{v}_{(1)}$, $\mathbf{w}_{(1)}$, $c_{(1)}$, $c_{(2)}$ could be obtained in terms of the expansions in Eq. (A26), but will turn out not to be required.

Using the general expressions for the determinant of block matrices [46] and Lemma 1, Eq. (A41) yields

$$\det \mathbf{F} = 1 + \varepsilon (\text{tr } \mathbf{B}_{(1)} + c_{(1)}) + \varepsilon^2 (\text{tr } \mathbf{B}_{(2)} + c_{(2)} + c_{(1)} \text{tr } \mathbf{B}_{(1)} + \det \mathbf{B}_{(1)} - \mathbf{w}_{(1)}^\top \mathbf{v}_{(1)}) + O(\varepsilon^3). \quad (\text{A43})$$

Moreover, from the general expression for the inverse of a block matrix [46],

$$\mathbf{F}^{-\top} = \left(\begin{array}{c|c} 1 + O(\varepsilon) & -\varepsilon \mathbf{w}_{(1)} + O(\varepsilon^2) \\ \hline O(\varepsilon) & 1 + O(\varepsilon) \end{array} \right), \quad (\text{A44})$$

and hence, recalling that $p = 1 + O(\varepsilon)$,

$$\mathbf{Q}_{(0)} = \mathbf{O}, \quad \mathbf{Q}_{(1)} \mathbf{N} = \left(\begin{array}{c} \mathbf{v}_{(1)} + \mathbf{w}_{(1)} \\ O(1) \end{array} \right). \quad (\text{A45})$$

As in Section II, $\mathbf{Q}_{(0)} = \mathbf{O}$ implies that, at leading order, Eq. (20) is $(\mathbf{Q}_{(1)} \mathbf{N})_{,Z^0} = 0$, with boundary condition $\mathbf{Q}_{(1)}^\dagger \mathbf{N} = \mathbf{0}$, which implies $\mathbf{Q}_{(1)} \mathbf{N} \equiv \mathbf{0}$. This and the incompressibility condition $\det \mathbf{F} = 1$ imply, from Eqs. (A43) and (A45),

$$c_{(1)} = -\text{tr } \mathbf{B}_{(1)}, \quad \mathbf{w}_{(1)} = -\mathbf{v}_{(1)}, \quad (\text{A46a})$$

and hence

$$c_{(2)} = -\text{tr } \mathbf{B}_{(2)} + (\text{tr } \mathbf{B}_{(1)})^2 - \det \mathbf{B}_{(1)} - \mathbf{v}_{(1)}^\top \mathbf{v}_{(1)}. \quad (\text{A46b})$$

e. Expansion of the constitutive relations

Before expanding the constitutive relations to obtain the asymptotic expansion of the three-dimensional energy density, we need to introduce one further result:

Lemma 4. *Let \mathbf{M}, \mathbf{N} be 2×2 matrices. Then*

$$(i) \quad \text{tr } (\mathbf{M}^2) = (\text{tr } \mathbf{M})^2 - 2 \det \mathbf{M},$$

$$(ii) \quad \text{tr } (\mathbf{M}^2 \mathbf{N}) = \text{tr } \mathbf{M} \text{tr } (\mathbf{M} \mathbf{N}) - \det \mathbf{M} \text{tr } \mathbf{N}.$$

Proof. The Cayley–Hamilton theorem [46] implies that, for a 2×2 matrix, $\mathbf{M}^2 = (\text{tr } \mathbf{M}) \mathbf{M} - (\det \mathbf{M}) \mathbf{I}$. Taking the trace on both sides of this relation and noting that $\text{tr } \mathbf{I} = 2$, we obtain (i). Multiplying this relation by \mathbf{N} and taking the trace yields (ii). \square

We start by computing the expansion of the (left) Cauchy–Green tensor: from Eq. (A41), we obtain

$$\mathbf{C} = \mathbf{F}^\top \mathbf{F} = \left(\begin{array}{c|c} 1 + \varepsilon (\mathbf{B}_{(1)} + \mathbf{B}_{(1)}^\top) + \varepsilon^2 (\mathbf{B}_{(2)} + \mathbf{B}_{(2)}^\top + \mathbf{B}_{(1)}^\top \mathbf{B}_{(1)} + \mathbf{w}_{(1)} \mathbf{w}_{(1)}^\top) + O(\varepsilon^3) & O(\varepsilon) \\ \hline O(\varepsilon) & 1 + 2\varepsilon c_{(1)} + \varepsilon^2 (2c_{(2)} + c_{(1)}^2 + \mathbf{v}_{(1)}^\top \mathbf{v}_{(1)}) + O(\varepsilon^3) \end{array} \right), \quad (\text{A47})$$

and hence, noting in particular that $\text{tr } (\mathbf{w}_{(1)} \mathbf{w}_{(1)}^\top) = \text{tr } (\mathbf{w}_{(1)} \mathbf{w}_{(1)}^\top)^\top = \mathbf{w}_{(1)}^\top \mathbf{w}_{(1)}$ since this expression is a scalar,

$$\begin{aligned} \mathcal{J}_1 = \text{tr } \mathbf{C} &= 3 + \varepsilon [2(\text{tr } \mathbf{B}_{(1)} + c_{(1)})] + \varepsilon^2 [2(\text{tr } \mathbf{B}_{(2)} + c_{(2)}) + \text{tr } (\mathbf{B}_{(1)}^\top \mathbf{B}_{(1)}) + c_{(1)}^2 + \mathbf{v}_{(1)}^\top \mathbf{v}_{(1)} + \mathbf{w}_{(1)}^\top \mathbf{w}_{(1)}] + O(\varepsilon^3) \\ &= 3 + \varepsilon^2 [3(\text{tr } \mathbf{B}_{(1)})^2 - 2 \det \mathbf{B}_{(1)} + \text{tr } (\mathbf{B}_{(1)}^\top \mathbf{B}_{(1)})] + O(\varepsilon^3) = 3 + \varepsilon^2 [2(\text{tr } \mathbf{B}_{(1)})^2 + \text{tr } (\mathbf{B}_{(1)}^\top \mathbf{B}_{(1)})] + O(\varepsilon^3), \end{aligned} \quad (\text{A48a})$$

where we have used, first, Eqs. (A46) and, second, Lemma 4. Using general properties of the trace operator, that for matrices \mathbf{M}, \mathbf{N} , $\text{tr } \mathbf{M}^\top = \text{tr } \mathbf{M}$ and $\text{tr } \mathbf{MN} = \text{tr } \mathbf{NM}$, yields an equivalent, more symmetric form of this result:

$$\mathcal{J}_1 - 3 = 2\varepsilon^2 \left[(\text{tr } \mathbf{e})^2 + \text{tr } (\mathbf{e}^2) \right] + O(\varepsilon^3), \quad \text{where } \mathbf{e} = \frac{\mathbf{B}_{(1)} + \mathbf{B}_{(1)}^\top}{2}, \quad (\text{A48b})$$

so that \mathbf{e} is the symmetric effective two-dimensional strain tensor. This determines the leading-order term in the expansion of the three-dimensional energy density e defined in Eq. (18), and thus completes the asymptotic expansion for the limit of a thin shell that undergoes general large bending deformations.

Some more simplifications are however possible in this general case. In what follows, we shall denote the symmetric part of a tensor \mathbf{M} using overlines, so that $\overline{\mathbf{M}} = (\mathbf{M} + \mathbf{M}^\top)/2$. Then, using Eqs. (A40) and (A42) and defining $\mathbf{J} = \mathbf{L}\lambda^0$, we obtain

$$\mathbf{e} = \overline{\mathbf{E}} + e_1 \overline{\mathbf{L}} + e_2 \overline{\mathbf{L} \text{adj } \lambda^0} + \left[e_3 \text{tr } \overline{\mathbf{E}} + e_5 \text{tr } \overline{\mathbf{L}} + e_7 \text{tr } \overline{\mathbf{J}} \right] \overline{\lambda^0} + \left[e_4 \text{tr } \overline{\mathbf{E}} + e_6 \text{tr } \overline{\mathbf{L}} + e_8 \text{tr } \overline{\mathbf{J}} \right] \mathbf{I}, \quad (\text{A49})$$

where

$$e_1 = \frac{Z^0}{1 + 2\mathcal{H}^0 Z^0 + \mathcal{K}^0 (Z^0)^2}, \quad e_2 = Z^0 e_1, \quad e_3 = -\frac{Z^0 + \mathcal{H}^0 (Z^0)^2 + \frac{1}{3}\mathcal{K}^0 (Z^0)^3}{\left[1 + 2\mathcal{H}^0 Z^0 + \mathcal{K}^0 (Z^0)^2 \right]^2}, \quad e_4 = \mathcal{K}^0 Z^0 e_3, \quad (\text{A50a})$$

$$e_5 = -\frac{\frac{1}{2}(Z^0)^2 + \frac{2}{3}\mathcal{H}^0 (Z^0)^3}{\left[1 + 2\mathcal{H}^0 Z^0 + \mathcal{K}^0 (Z^0)^2 \right]^2}, \quad e_6 = \mathcal{K}^0 Z^0 e_5, \quad e_7 = \frac{\frac{1}{3}(Z^0)^3}{\left[1 + 2\mathcal{H}^0 Z^0 + \mathcal{K}^0 (Z^0)^2 \right]^2}, \quad e_8 = \mathcal{K}^0 Z^0 e_7. \quad (\text{A50b})$$

Now, on applying Lemmata 3 and 4 repeatedly, we obtain, from Eq. (A49),

$$\text{tr } \mathbf{e} = \left(1 + 2\mathcal{H}^0 e_3 + 2e_4 \right) \text{tr } \overline{\mathbf{E}} + \left(e_1 + 2\mathcal{H}^0 e_2 + 2\mathcal{H}^0 e_5 + 2e_6 \right) \text{tr } \overline{\mathbf{L}} + \left(2\mathcal{H}^0 e_7 + 2e_8 - e_2 \right) \text{tr } \overline{\mathbf{J}}, \quad (\text{A51a})$$

$$\begin{aligned} \text{tr } \mathbf{e}^2 = & \text{tr } \overline{\mathbf{E}}^2 + (e_1 + 2e_2\mathcal{H}^0)^2 \text{tr } \overline{\mathbf{L}}^2 + e_2^2 \text{tr } \overline{\mathbf{J}}^2 + 2(e_1 + 2e_2\mathcal{H}^0) \text{tr } \overline{\mathbf{E}} \overline{\mathbf{L}} - 2e_2 \text{tr } \overline{\mathbf{E}} \overline{\mathbf{J}} - 2e_2(e_1 + 2e_2\mathcal{H}^0) \text{tr } \overline{\mathbf{L}} \overline{\mathbf{J}} \\ & + 2 \left\{ e_4 + (e_4 + e_3\mathcal{H}^0)^2 + \left[(\mathcal{H}^0)^2 - \mathcal{K}^0 \right] e_3^2 \right\} (\text{tr } \overline{\mathbf{E}})^2 + 2 \left\{ (e_8 + e_7\mathcal{H}^0)^2 + e_1 e_7 - e_2 e_8 + \left[(\mathcal{H}^0)^2 - \mathcal{K}^0 \right] e_7^2 \right\} (\text{tr } \overline{\mathbf{J}})^2 \\ & + 2 \left\{ e_6(e_1 + 2e_2\mathcal{H}^0) + (e_6 + e_5\mathcal{H}^0)^2 + e_2 e_5 \mathcal{K}^0 + \left[(\mathcal{H}^0)^2 - \mathcal{K}^0 \right] e_5^2 \right\} (\text{tr } \overline{\mathbf{L}})^2 + 2e_3 \text{tr } \overline{\mathbf{E}} \text{tr } \overline{\mathbf{J}} + 2e_5 \text{tr } \overline{\mathbf{L}} \text{tr } \overline{\mathbf{J}} \\ & + 2 \left\{ 2(e_4 + e_3\mathcal{H}^0)(e_6 + e_5\mathcal{H}^0) + e_4(e_1 + 2e_2\mathcal{H}^0) + e_6 + e_2 e_3 \mathcal{K}^0 + 2 \left[(\mathcal{H}^0)^2 - \mathcal{K}^0 \right] e_3 e_5 \right\} \text{tr } \overline{\mathbf{E}} \text{tr } \overline{\mathbf{L}} \\ & + 2 \left\{ 2(e_4 + e_3\mathcal{H}^0)(e_8 + e_7\mathcal{H}^0) + e_8 + e_1 e_3 - e_2 e_4 + 2 \left[(\mathcal{H}^0)^2 - \mathcal{K}^0 \right] e_3 e_7 \right\} \text{tr } \overline{\mathbf{E}} \text{tr } \overline{\mathbf{J}} \\ & + 2 \left\{ 2(e_6 + e_5\mathcal{H}^0)(e_8 + e_7\mathcal{H}^0) + e_8(e_1 + 2e_2\mathcal{H}^0) + e_1 e_5 - e_2 e_6 + 2 \left[(\mathcal{H}^0)^2 - \mathcal{K}^0 \right] e_5 e_7 \right\} \text{tr } \overline{\mathbf{L}} \text{tr } \overline{\mathbf{J}}, \end{aligned} \quad (\text{A51b})$$

where we have set $\Xi = \mathbf{E}\lambda^0$ and used the symmetry of \mathbf{L} and λ^0 . On substitution in Eq. (A48b), these yield a more explicit expression for the leading-order three-dimensional elastic energy density e . We are not aware of any more possible simplifications of the traces in these expressions in the general case; we note that the coefficients of the different trace terms in Eqs. (A51) only depend on the intrinsic configuration.

f. Averaging over the transverse coordinate

The volume element in the intrinsic configuration \mathcal{V}^0 is, by definition and using Eq. (A20b),

$$\begin{aligned} dV^0 &= \sqrt{\det \mathbf{G}^0} \left(\frac{dS}{\sqrt{g}} \right) d\zeta \\ &= \varepsilon \left[1 + 2\mathcal{H}^0 Z^0 + \mathcal{K}^0 (Z^0)^2 \right] dS dZ^0 \end{aligned} \quad (\text{A52})$$

where dS is the surface element of the undeformed midsurface \mathcal{S} , and hence the elastic energy of the shell is

$$\mathcal{E} = \int_{\mathcal{S}} \hat{e} dS, \quad (\text{A53a})$$

in which expression

$$\hat{e} = \varepsilon \int_{-H^0/2}^{H^0/2} e(Z^0) \left[1 + 2\mathcal{H}^0 Z^0 + \mathcal{K}^0 (Z^0)^2 \right] dZ^0, \quad (\text{A53b})$$

is the effective two-dimensional energy density. In this expression, H^0 is given in terms of the undeformed thickness h of the shell by Eq. (A22b).

Since the coefficients functions $e_1, e_2, e_3, e_4, e_5, e_6, e_7, e_8$ defined in Eqs. (A50) that appear in Eq. (A49) and hence in the expansion of e are rational functions of Z^0 , the integral with respect to Z^0 in Eq. (A53b) can be performed in closed form, but the resulting expressions are, in the general case, extremely

cumbersome and therefore not presented here. For this reason, the general theory presented here is likely most useful to describe deformations with some additional symmetry, such as the axisymmetric deformations discussed in Section II.

APPENDIX B: DERIVATION OF THE GOVERNING EQUATIONS FOR AXISYMMETRIC DEFORMATIONS

In this Appendix, we derive the governing equations for axisymmetric deformations, by varying the elastic the elastic energy (47a). Similar derivations are given in our previous work [9, 10] for the elastic theories considered there, but here, we keep the explicit asymptotic scalings in the derivation. From Eq. (47b), with the alternative curvature strains defined in Eq. (51b) and considering leading-order terms only, we have

$$\delta \hat{e} = \varepsilon (n_s \delta E_s + n_\phi \delta E_\phi) + m_s \delta K_s + m_\phi \delta K_\phi, \quad (\text{B1})$$

wherein the shell stresses and shell moments are

$$n_s = C\varepsilon^2 h [\alpha_{ss} E_s + \alpha_{s\phi} E_\phi + h (\beta_{ss} K_s + \beta_{s\phi} K_\phi)], \quad (\text{B2a})$$

$$n_\phi = C\varepsilon^2 h [\alpha_{\phi s} E_s + \alpha_{\phi\phi} E_\phi + h (\beta_{\phi s} K_s + \beta_{\phi\phi} K_\phi)], \quad (\text{B2b})$$

$$m_s = C\varepsilon^3 h^2 [\beta_{ss} E_s + \beta_{s\phi} E_\phi + h (\gamma_{ss} K_s + \gamma_{s\phi} K_\phi)], \quad (\text{B2c})$$

$$m_\phi = C\varepsilon^3 h^2 [\beta_{s\phi} E_s + \beta_{\phi\phi} E_\phi + h (\gamma_{\phi s} K_s + \gamma_{\phi\phi} K_\phi)], \quad (\text{B2d})$$

since $\alpha_{s\phi} = \alpha_{\phi s}$, $\gamma_{s\phi} = \gamma_{\phi s}$. Now, from the definitions of the shell and curvature strains in Eqs. (50) and (51b),

$$\delta E_s = \frac{\sec \tilde{\psi} \delta \tilde{r}' + f_s \tan \tilde{\psi} \delta \tilde{\psi}}{\varepsilon f_s^0}, \quad \delta E_\phi = \frac{1}{\varepsilon f_\phi^0} \left(\frac{\delta \tilde{r}}{r} \right), \quad (\text{B3a})$$

and

$$\delta K_s = \frac{\tilde{\psi}'}{(f_s^0)^2 f_\phi^0}, \quad \delta K_\phi = \frac{1}{f_s^0 (f_\phi^0)^2} \left(\frac{\cos \psi}{r} \delta \psi \right). \quad (\text{B3b})$$

Hence, on letting

$$N_s = \frac{n_s}{f_\phi f_s^0}, \quad N_\phi = \frac{n_\phi}{f_s f_\phi^0}, \quad (\text{B4a})$$

$$M_s = \frac{m_s}{f_\phi (f_s^0)^2 f_\phi^0}, \quad M_\phi = \frac{m_\phi}{f_s f_s^0 (f_\phi^0)^2}, \quad (\text{B4b})$$

we obtain, from Eq. (47a) and using Eq. (9),

$$\begin{aligned} \frac{\delta \mathcal{E}}{2\pi} &= [\tilde{r} N_s \sec \tilde{\psi} \delta \tilde{r} + \tilde{r} M_s \delta \tilde{\psi}] \\ &- \int_{\mathcal{C}} \left[\frac{d}{ds} (\tilde{r} M_s) - \tilde{r} f_s N_s \tan \tilde{\psi} - f_s M_\phi \cos \tilde{\psi} \right] ds \\ &- \int_{\mathcal{C}} \left[\frac{d}{ds} (\tilde{r} N_s \sec \tilde{\psi}) - f_s N_\phi \right] ds, \end{aligned} \quad (\text{B5})$$

from which we read off the governing equations and boundary conditions.

As in standard shell theories [23], the apparent singularity in the resulting equations is removed by introducing the

transverse shear tension, $T = -N_s \tan \tilde{\psi}$, and we obtain, using Eqs. (10) and (13),

$$\frac{dN_s}{ds} = f_s \left(\frac{N_\phi - N_s}{\tilde{r}} \cos \tilde{\psi} + \kappa_s T \right), \quad (\text{B6a})$$

$$\frac{dM_s}{ds} = f_s \left(\frac{M_\phi - M_s}{\tilde{r}} \cos \tilde{\psi} - T \right). \quad (\text{B6b})$$

Moreover, by differentiating the definition of T and using Eq. (B6a), we find

$$\frac{dT}{ds} = -f_s \left(\kappa_s N_s + \kappa_\phi N_\phi + T \frac{\cos \tilde{\psi}}{\tilde{r}} \right). \quad (\text{B6c})$$

Together with the relations

$$\frac{d\tilde{r}}{ds} = f_s \cos \tilde{\psi}, \quad \frac{d\tilde{\psi}}{ds} = f_s \kappa_s \quad (\text{B7})$$

from Eqs. (10) and (13), Eqs. (B6) determine the deformed configuration of the shell. Having solved these equations, integrating the otherwise redundant shape equation $\tilde{z}' = f_s \sin \tilde{\psi}$ from Eqs. (10) yields the shape of the shell.

Numerical solution of Eqs. (B6)

We conclude the derivation of the governing equations for axisymmetric deformations with two remarks on the numerical solution of Eqs. (B6).

First, we note that Eqs. (B6) are singular where $\tilde{r} = 0$. At such a point, geometric continuity implies $\tilde{\psi} = 0$. Hence $T = 0$ there by definition, and $N_\phi = N_s$ for regularity in Eq. (B6a). Moreover, by applying l'Hôpital's rule to the definitions in Eqs. (9) and (13), $f_s = f_\phi$, $\kappa_s = \kappa_\phi$. Hence Eqs. (B6) are replaced with

$$\frac{dN_s}{ds} = 0, \quad \frac{dM_s}{ds} = 0, \quad \frac{dT}{ds} = -f_s \kappa_s N_s, \quad (\text{B8})$$

of which the first two follow by reflection across the axis of symmetry, and the last follows by applying l'Hôpital's rule to Eq. (B6c) and using the previous observations and Eqs. (B7).

Second, as discussed also in Ref. [9, 10], at each stage of the numerical solution, $f_s, f_\phi, \kappa_s, \kappa_\phi$ must be determined from $\tilde{r}, \tilde{\psi}, M_s, N_s$. To begin with, f_ϕ, κ_ϕ and hence E_ϕ, K_ϕ are computed directly from $\tilde{r}, \tilde{\psi}$ using the definitions (50) and (51b). We can then compute f_s, κ_s by noting that, once f_ϕ, E_ϕ, K_ϕ are known, the definitions of N_s, M_s in Eqs. (B2a), (B2c), and (B4) define a system of linear equations for E_s, K_s . Their definitions (50) and (51b) then yield f_s and finally κ_s . We can then compute N_ϕ, M_ϕ using Eqs. (B2b), (B2d), and (B4), and thus continue the numerical integration. (Moreover, if $\tilde{r} = 0$, we similarly obtain two linear equations for $f = f_s = f_\phi$ and $k = f_s \kappa_s = f_\phi \kappa_\phi$, from the solution of which the numerical integration can be continued.)

APPENDIX C: NEO-HOOKEAN RELATIONS AS THE THIN SHELL LIMIT OF GENERAL CONSTITUTIVE RELATIONS

In this final Appendix, we show that the effective two-dimensional constitutive relations, resulting from Eq. (A48b),

$$e = C\varepsilon^2 \left[(\text{tr } \mathbf{e})^2 + \text{tr } (\mathbf{e}^2) \right] + O(\varepsilon^3), \quad (\text{C1})$$

are general and do not only apply for the neo-Hookean three-dimensional constitutive relations assumed in Eq. (18). To this end, following Ref. [21], we consider energy densities expressible as a general power series

$$e = \frac{1}{2} \sum_{m=0}^{\infty} \sum_{n=0}^{\infty} C_{mn} (\mathcal{I}_1 - 3)^m (\mathcal{I}_2 - 3)^n, \quad (\text{C2})$$

where we set $C_{00} = 0$ without loss of generality, and where $\mathcal{I}_1 = \text{tr } \mathbf{C}$ as before and $\mathcal{I}_2 = \text{tr } \mathbf{C}^2$ is the second invariant of the Cauchy–Green tensor $\mathbf{C} = (\mathbf{R}\mathbf{F})^\top (\mathbf{R}\mathbf{F}) = \mathbf{F}^\top \mathbf{F}$. In this expression, \mathbf{R} is, in the notation of Appendix A, the rotation that maps \mathcal{B}^0 onto $\tilde{\mathcal{B}}^0$, so that $\mathbf{R}^\top \mathbf{R} = \mathbf{I}$. Using results from Ref. [21] and continuing to use the notation of Appendix A, the Piola–Kirchhoff stress tensor for this material is, with respect to $\mathcal{B}^0 \otimes (\mathcal{B}^0)^*$,

$$\mathbf{P} = 2 \left\{ e_{,\mathcal{I}_1} (\mathbf{R}\mathbf{F}) + e_{,\mathcal{I}_2} \left[\mathcal{I}_1 (\mathbf{R}\mathbf{F}) - (\mathbf{R}\mathbf{F})(\mathbf{R}\mathbf{F})^\top (\mathbf{R}\mathbf{F}) \right] \right\} - p(\mathbf{R}\mathbf{F})^{-\top} = \mathbf{R}\mathbf{Q}, \quad (\text{C3a})$$

with

$$\mathbf{Q} = 2 \left[e_{,\mathcal{I}_1} \mathbf{F} + e_{,\mathcal{I}_2} (\mathcal{I}_1 \mathbf{F} - \mathbf{F}\mathbf{C}) \right] - P\mathbf{F}^{-\top}, \quad (\text{C3b})$$

since $\mathbf{R}^\top \mathbf{R} = \mathbf{I}$, and where \mathbf{F} is given by Eq. (A14b), and we recall that $\mathbf{C} = \mathbf{F}^\top \mathbf{F}$, and where $P = P_{(0)} + O(\varepsilon)$ is pressure. (We now use an uppercase letter to denote pressure to emphasise that it is scaled differently to Appendix A; in the notation used there, $P = Cp$.)

(Partial) solution at order $O(1)$. From Eq. (A14b), we compute the leading-order expansion of \mathbf{C} , finding

$$\mathbf{C} = \left(\frac{\mathbf{B}^\top \mathbf{B} + \mathbf{w}\mathbf{w}^\top}{\mathbf{v}^\top \mathbf{B} + c\mathbf{w}^\top} \middle| \frac{\mathbf{B}^\top \mathbf{v} + c\mathbf{w}}{\mathbf{v}^\top \mathbf{v} + c^2} \right) + O(\varepsilon), \quad (\text{C4})$$

and hence $\mathcal{I}_1 = \text{tr } (\mathbf{B}^\top \mathbf{B}) + \mathbf{w}^\top \mathbf{w} + \mathbf{v}^\top \mathbf{v} + c^2 + O(\varepsilon)$. Writing $e_{,\mathcal{I}_1} = E_1 + O(\varepsilon)$, $e_{,\mathcal{I}_2} = E_2 + O(\varepsilon)$, and using the expansion (A29) of the incompressibility condition, we find

$$\mathbf{Q} = \left(\begin{array}{c|c} O(1) & 2 \left\{ E_1 + E_2 \left[\text{tr } (\mathbf{B}^\top \mathbf{B}) + \mathbf{w}^\top \mathbf{w} \right] \right\} \mathbf{v} \\ & - 2E_2 \mathbf{B}\mathbf{B}^\top \mathbf{w} - 2E_2 c \mathbf{B}\mathbf{w} \\ & + P_{(0)} (\det \mathbf{B}) \mathbf{B}^{-\top} \mathbf{w} \\ \hline O(1) & 2c \left[E_1 + E_2 \text{tr } (\mathbf{B}^\top \mathbf{B}) \right] \\ & - 2E_2 \mathbf{w}^\top \mathbf{B}^\top \mathbf{v} - P_{(0)} \det \mathbf{B} \end{array} \right) + O(\varepsilon). \quad (\text{C5})$$

The boundary conditions imply $\mathbf{Q}\mathbf{N} = O(\varepsilon)$ as in Appendix A, and hence, from Eqs. (A29) and (C5), the leading-order problem is

$$c - \mathbf{w}^\top \mathbf{B}^{-1} \mathbf{v} = (\det \mathbf{B})^{-1}, \quad (\text{C6a})$$

$$2 \left\{ E_1 + E_2 \left[\text{tr } (\mathbf{B}^\top \mathbf{B}) + \mathbf{w}^\top \mathbf{w} \right] \right\} \mathbf{v} - 2E_2 \mathbf{B}\mathbf{B}^\top \mathbf{w} - 2E_2 c \mathbf{B}\mathbf{w} + P_{(0)} (\det \mathbf{B}) \mathbf{B}^{-\top} \mathbf{w} = \mathbf{0}, \quad (\text{C6b})$$

$$2c \left[E_1 + E_2 \text{tr } (\mathbf{B}^\top \mathbf{B}) \right] - 2E_2 \mathbf{w}^\top \mathbf{B}^\top \mathbf{v} - P_{(0)} \det \mathbf{B} = 0. \quad (\text{C6c})$$

These equations have a trivial solution

$$Z_{(0)} \equiv 0, \quad \mathbf{S}_{(0)} \equiv \mathbf{0}, \quad P_{(0)} = C_{10} + 2C_{01}, \quad (\text{C7})$$

for which $\mathbf{B} = \mathbf{I}$, $\mathbf{v} = \mathbf{w} = \mathbf{0}$, $c = 1$, and hence $\mathbf{C} = \mathbf{I} + O(\varepsilon)$, so that $\mathcal{I}_1 = \mathcal{I}_2 = 3 + O(\varepsilon)$ and thus $E_1 = C_{10}/2$, $E_2 = C_{01}/2$. We were not however able to show that this is the only solution of the nonlinear first-order differential equations for $Z_{(0)}$, $\mathbf{S}_{(0)}$ as functions of Z^0 provided by Eqs. (C6) that satisfies the conditions $Z_{(0)} = 0$, $\mathbf{S}_{(0)} = \mathbf{0}$ on $Z^0 = 0$. In this respect, our solution of the leading-order problem remains partial.

Our failure to solve Eqs. (C6) emphasises once again that what distinguishes these problems of large bending deformations from classical problems in elastic shell theories is the fact that the leading-order problem for these deformations is not trivial. In fact, were a second solution of Eqs. (C6) to exist, global energy considerations would select the solution; this would open a new can of worms in the analysis.

Solution at order $O(\varepsilon)$. At this stage, we take Eqs. (C7) as the solution of the leading-order problem (C6) and proceed thence. The expansion (A41) of the deformation gradient thus still holds true, and we deduce

$$\mathbf{C} = \left(\frac{\mathbf{I} + \varepsilon (\mathbf{B}_{(1)} + \mathbf{B}_{(1)}^\top)}{\varepsilon (\mathbf{v}_{(1)}^\top + \mathbf{w}_{(1)}^\top)} \middle| \frac{\varepsilon (\mathbf{v}_{(1)} + \mathbf{w}_{(1)})}{1 + 2\varepsilon c_{(1)}} \right) + O(\varepsilon^2), \quad (\text{C8a})$$

$$\mathbf{C}^2 = \left(\frac{\mathbf{I} + 2\varepsilon (\mathbf{B}_{(1)} + \mathbf{B}_{(1)}^\top)}{O(\varepsilon)} \middle| \frac{O(\varepsilon)}{1 + 4\varepsilon c_{(1)}} \right) + O(\varepsilon^2), \quad (\text{C8b})$$

and thence

$$\mathcal{I}_1 = 3 + \varepsilon [2(\text{tr } \mathbf{B}_{(1)} + c_{(1)})] + O(\varepsilon^2), \quad (\text{C9a})$$

$$\mathcal{I}_2 = 3 + \varepsilon [4(\text{tr } \mathbf{B}_{(1)} + c_{(1)})] + O(\varepsilon^2), \quad (\text{C9b})$$

But, from Eq. (A43), $1 = \det \mathbf{F} = 1 + \varepsilon (\text{tr } \mathbf{B}_{(1)} + c_{(1)}) + O(\varepsilon^2)$, so $c_{(1)} = -\text{tr } \mathbf{B}_{(1)}$, and hence $\mathcal{I}_1 = \mathcal{I}_2 = 3 + O(\varepsilon^2)$. Hence

$$e = \frac{1}{2} [C_{10} (\mathcal{I}_1 - 3) + C_{01} (\mathcal{I}_2 - 3)] + O(\varepsilon^4), \quad (\text{C10})$$

and, in particular, $e_{,\mathcal{I}_1} = C_{10}/2 + O(\varepsilon^2)$, $e_{,\mathcal{I}_2} = C_{01}/2 + O(\varepsilon^2)$. In this way, the constitutive relations have reduced to those of a Mooney–Rivlin solid [17]. We then obtain

$$\mathbf{Q}_{(0)} = \mathbf{0}, \quad \mathbf{Q}_{(1)} \mathbf{N} = (C_{10} + C_{01}) \left(\frac{\mathbf{v}_{(1)} + \mathbf{w}_{(1)}}{O(1)} \right), \quad (\text{C11})$$

where we have used $P = C_{10} + 2C_{01} + O(\varepsilon)$. As in Appendix A, the boundary conditions lead to $\mathbf{Q}_{(1)} \mathbf{N} = \mathbf{0}$. It follows that Eqs. (A46a) still hold.

Solution at order $O(\varepsilon^2)$. Since the expansion (A43) of the incompressibility condition is independent of the constitutive relations and therefore still holds, Eqs. (A46a) still imply Eq. (A46b) and hence Eq. (A48b). Eqs. (A46a) and (C8a) then show that the off-diagonal terms in Eq. (A47) are in fact of order $O(\varepsilon^2)$. It then follows from Eq. (A47) that

$$\begin{aligned} \mathcal{I}_2 = \text{tr} \left\{ \left[\mathbf{I} + \varepsilon (\mathbf{B}_{(1)} + \mathbf{B}_{(1)}^\top) + \varepsilon^2 (\mathbf{B}_{(2)} + \mathbf{B}_{(2)}^\top) \right. \right. \\ \left. \left. + \mathbf{B}_{(1)}^\top \mathbf{B}_{(1)} + \mathbf{w}_{(1)} \mathbf{w}_{(1)}^\top \right] + O(\varepsilon^3) \right\}^2 \\ + \left[1 + 2\varepsilon c_{(1)} + \varepsilon^2 (2c_{(2)} + c_{(1)}^2 + \mathbf{v}_{(1)}^\top \mathbf{v}_{(1)}) + O(\varepsilon^3) \right]^2 \\ + O(\varepsilon^4). \end{aligned} \quad (\text{C12a})$$

We have shown above that $\mathcal{J}_2 = 3 + O(\varepsilon^2)$. Using Eqs. (A46) and Lemma 4, we now find

$$\begin{aligned}\mathcal{J}_2 - 3 &= 2\varepsilon^2 \left[2(\text{tr } \mathbf{B}_{(2)} + c_{(2)}) + \mathbf{w}_{(1)}^\top \mathbf{w}_{(1)} + \mathbf{v}_{(1)}^\top \mathbf{v}_{(1)} \right. \\ &\quad \left. + \text{tr } (\mathbf{B}_{(1)}^2) + 2 \text{tr } (\mathbf{B}_{(1)}^\top \mathbf{B}_{(1)}) + 2c_{(1)}^2 \right] + O(\varepsilon^3) \\ &= 4\varepsilon^2 \left[2(\text{tr } \mathbf{B}_{(1)})^2 + \text{tr } (\mathbf{B}_{(1)}^2) + \text{tr } (\mathbf{B}_{(1)}^\top \mathbf{B}_{(1)}) \right] + O(\varepsilon^3) \\ &= 4(\mathcal{J}_1 - 3) + O(\varepsilon^3).\end{aligned}\quad (\text{C12b})$$

by comparison with Eq. (A48a). Hence, from Eq. (C10),

$$e = \frac{C}{2}(\mathcal{J}_1 - 3) + O(\varepsilon^3), \quad \text{with } C = C_{10} + 4C_{01}. \quad (\text{C13})$$

Up to smaller corrections, these are the neo-Hookean constitutive relations assumed in Eq. (18) and throughout Section II and Appendix A, and which, as shown there, indeed reduce at order $O(\varepsilon^2)$ to the effective two-dimensional relations (C1). Assuming that the trivial solution (C7) of the leading-order problem Eq. (C6) is unique, this proves our claim in Section IV, that these effective two-dimensional constitutive relations are general.

-
- [1] R. Keller, L. A. Davidson, and D. R. Shook, How we are shaped: The biomechanics of gastrulation, *Differentiation* **71**, 171 (2003).
 - [2] M. Leptin, Gastrulation movements: the logic and the nuts and bolts, *Dev. Cell* **8**, 305 (2005).
 - [3] T. Lecuit and P.-F. Lenne, Cell surface mechanics and the control of cell shape, tissue patterns and morphogenesis, *Nat. Rev. Mol. Cell Biol.* **8**, 633 (2007).
 - [4] R. Keller and D. Shook, The bending of cell sheets - from folding to rolling, *BMC Biol.* **9**, 90 (2011).
 - [5] T. Lecuit, P.-F. Lenne, and E. Munro, Force generation, transmission, and integration during cell and tissue morphogenesis, *Ann. Rev. Cell Dev. Biol.* **27**, 157 (2011).
 - [6] M. Tada and C.-P. Heisenberg, Convergent extension: using collective cell migration and cell intercalation to shape embryos, *Development* **139**, 3897 (2012).
 - [7] S. Höhn, A. R. Honerkamp-Smith, P. A. Haas, P. Khuc Trong, and R. E. Goldstein, Dynamics of a *Volvox* embryo turning itself inside out, *Phys. Rev. Lett.* **114**, 178101 (2015).
 - [8] P. A. Haas and R. E. Goldstein, Elasticity and glocality: Initiation of embryonic inversion in *Volvox*, *J. R. Soc. Interface* **12**, 20150671 (2015).
 - [9] P. A. Haas, S. S. M. H. Höhn, A. R. Honerkamp-Smith, J. B. Kirkegaard, and R. E. Goldstein, The noisy basis of morphogenesis: mechanisms and mechanics of cell sheet folding inferred from developmental variability, *PLoS Biol.* **16**, e2005536 (2018).
 - [10] P. A. Haas and R. E. Goldstein, Embryonic inversion in *Volvox carteri*: The flipping and peeling of elastic lips, *Phys. Rev. E* **98**, 052415 (2018).
 - [11] N. C. Heer, P. W. Miller, S. Chanet, N. Stoop, J. Dunkel, and A. C. Martin, Actomyosin-based tissue folding requires a multicellular myosin gradient, *Development* **144**, 1876 (2017).
 - [12] H. G. Yevick, P. W. Miller, J. Dunkel, and A. C. Martin, Structural redundancy in supracellular actomyosin networks enables robust tissue folding, *Dev. Cell* **50**, 586 (2019).
 - [13] P. W. Miller, N. Stoop, and J. Dunkel, Geometry of wave propagation on active deformable surfaces, *Phys. Rev. Lett.* **120**, 268001 (2018).
 - [14] P. G. Ciarlet, An introduction to differential geometry with applications to elasticity, *J. Elasticity* **78**, 1 (2005).
 - [15] B. Audoly and Y. Pomeau, *Elasticity and Geometry* (Oxford University Press, Oxford, United Kingdom, 2010) Chap. 12, pp. 435–453 and App. D, pp. 571–581.
 - [16] D. J. Steigmann, Koiter's shell theory from the perspective of three-dimensional nonlinear elasticity, *J. Elasticity* **111**, 91 (2013).
 - [17] A. Goriely, *The Mathematics and Mechanics of Biological Growth* (Springer, Berlin, Germany, 2017) Chap. 11 & 12, pp. 261–373.
 - [18] D. Ambrosi, M. Ben Amar, C. J. Cyron, A. De Simone, A. Goriely, J. D. Humphrey, and E. Kuhl, Growth and remodelling of living tissues: perspectives, challenges and opportunities, *J. R. Soc. Interface* **16**, 20190233 (2019).
 - [19] E. K. Rodriguez, A. Hoger, and A. D. McCulloch, Stress-dependent finite growth in soft elastic tissues, *J. Biomech.* **27**, 455 (1994).
 - [20] J. Dervaux and M. Ben Amar, Morphogenesis of growing soft tissues, *Phys. Rev. Lett.* **101**, 068101 (2008).
 - [21] J. Dervaux, P. Ciarletta, and M. Ben Amar, Morphogenesis of thin hyperelastic plates: A constitutive theory of biological growth in the Föppl–von Kármán limit, *J. Mech. Phys. Solids* **57**, 458 (2009).
 - [22] E. Ventsel and T. Krauthammer, *Thin plates and shells: theory, analysis, and applications* (Marcel Dekker, New York, NY, 2001) Chap. 12, pp. 325–347.
 - [23] A. Libai and J. G. Simmonds, *The Nonlinear Theory of Elastic Shells*, 2nd ed. (Cambridge University Press, Cambridge, United Kingdom, 2005) Chap. V, pp. 159–342.
 - [24] V. Conte, F. Ulrich, B. Baum, J. Muñoz, J. Veldhuis, W. Brodland, and M. Miodownik, A biomechanical analysis of ventral furrow formation in the *Drosophila melanogaster* embryo, *PLoS One* **7**, e34473 (2012).
 - [25] A. Hallmann, Morphogenesis in the family Volvocaceae: Different tactics for turning an embryo right-side out, *Protist* **157**, 445 (2006).
 - [26] S. Höhn and A. Hallmann, There is more than one way to turn a spherical cellular monolayer inside out: type B embryo inversion in *Volvox globator*, *BMC Biol.* **9**, 89 (2011).
 - [27] Expansions were carried out using MATHEMATICA (Wolfram, Inc.) to assist with manipulating the complicated algebraic expressions that arise in these calculations.
 - [28] E. J. Doedel, B. E. Oldman, A. R. Champneys, F. Dercole, T. Fairgrieve, Y. Kuznetsov, R. Paffenroth, B. Sandstede, X. Wang, and C. Zhang, *Auto-07p: Continuation and Bifurcation Software for Ordinary Differential Equations*, Tech. Rep. (Concordia University, Montreal, Canada, 2012).
 - [29] M. Pezzulla, N. Stoop, X. Jiang, and D. P. Holmes, Curvature-driven morphing of non-Euclidean shells, *Proc. R. Soc. A* **473**,

20170087 (2017).

- [30] J. N. Reddy, *Theory and analysis of elastic plates and shells*, 2nd ed. (CRC Press, Boca Raton, FL, 2007) Chap. 10, pp. 359–402.
- [31] D. L. Kirk, *Volvox: molecular-genetic origins of multicellularity and cellular differentiation* (Cambridge University Press, Cambridge, United Kingdom, 1998).
- [32] D. L. Kirk, A twelve-step program for evolving multicellularity and a division of labor, *BioEssays* **27**, 299 (2005).
- [33] M. D. Herron, Origins of multicellular complexity: *Volvox* and the volvocine algae, *Mol. Ecol.* **25**, 1213 (2016).
- [34] R. E. Goldstein, Green algae as model organisms for biological fluid dynamics, *Annu. Rev. Fluid Mech.* **47**, 343 (2015).
- [35] D. L. Kirk and I. Nishii, *Volvox carteri* as a model for studying the genetic and cytological control of morphogenesis, *Dev. Growth Differ.* **43**, 621 (2001).
- [36] G. Matt and J. Umen, *Volvox*: A simple algal model for embryogenesis, morphogenesis and cellular differentiation, *Dev. Biol.* **419**, 99 (2016).
- [37] A. G. Desnitskiy, Comparative analysis of embryonic inversion in algae of the genus *Volvox* (Volvocales, Chlorophyta), *Russ. J. Dev. Biol.* **49**, 129 (2018).
- [38] W. J. Cooper and R. C. Albertson, Quantification and variation in experimental studies of morphogenesis, *Dev. Biol.* **321**, 295 (2008).
- [39] A. C. Oates, N. Gorfinkel, M. González-Gaitán, and C.-P. Heisenberg, Quantitative approaches in developmental biology, *Nature Rev. Gen.* **10**, 517 (2009).
- [40] L. A. Mihai, L. Chin, P. A. Janmey, and A. Goriely, A comparison of hyperelastic constitutive models applicable to brain and fat tissues, *J. R. Soc. Interface* **12**, 20150486 (2015).
- [41] L. A. Mihai, S. Budday, G. A. Holzapfel, E. Kuhl, and A. Goriely, A family of hyperelastic models for human brain tissue, *J. Mech. Phys. Solids* **106**, 60 (2017).
- [42] S. Budday, G. Sommer, C. Birkl, C. Langkammer, J. Haybaeck, J. Kohnert, M. Bauer, F. Paulsen, P. Steinmann, E. Kuhl, and G. A. Holzapfel, Mechanical characterization of human brain tissue, *Acta Biomater.* **48**, 319 (2017).
- [43] H. A. Erbay, On the asymptotic membrane theory of thin hyperelastic plates, *Int. J. Eng. Sci.* **35**, 151 (1997).
- [44] P. A. Haas and R. E. Goldstein, Nonlinear and nonlocal elasticity in coarse-grained differential-tension models of epithelia, *Phys. Rev. E* **99**, 022411 (2019).
- [45] E. Kreyszig, *Differential Geometry* (Dover, New York, NY, 1991) Chap. 4, pp. 118–153.
- [46] D. S. Bernstein, *Matrix Mathematics: Theory, Facts, and Formulas*, 2nd ed. (Princeton University Press, Princeton, NJ, 2009) Chap. 2.8, pp. 115–119 and Chap. 4.4, pp. 261–267.